STABILITY ANALYSIS AND ERROR ESTIMATE OF THE EXPLICIT SINGLE STEP TIME MARCHING DISCONTINUOUS GALERKIN METHOD WITH STAGE-DEPENDENT NUMERICAL FLUX PARAMETERS FOR A LINEAR HYPERBOLIC EQUATION IN ONE DIMENSION

YUAN XU*, CHI-WANG SHU†, AND QIANG ZHANG‡

Abstract. In this paper, we present the L^2-norm stability analysis and error estimates for the explicit single-step time marching discontinuous Galerkin (DG) method with stage-dependent flux parameters, when solving a linear constant-coefficient hyperbolic equation in one dimension. Two well-known examples of this method include the Runge–Kutta DG method with the downwind treatment for the negative time marching coefficients, as well as the Lax–Wendroff DG method with arbitrary numerical flux parameters to deal with the auxiliary variables. The stability analysis framework is an extension and an application of the matrix transferring process based on the temporal differences of stage solutions, and a new concept, named as the averaged numerical flux parameter, is proposed to reveal the essential numerical viscosity in the fully discrete status. Distinguished from the traditional analysis, we have to present a novel way to obtain the optimal error estimate in both space and time. The main tool is a series of space-time approximation functions for a given spatial function, which preserve the local structure of the fully discrete schemes and the balance of exact evolution under the control of the partial differential equation. Finally some numerical experiments are given to validate the theoretical results proposed in this paper.

Key words. discontinuous Galerkin method, explicit single step time marching, stage-dependent numerical flux parameters, hyperbolic equation, stability analysis and error estimate

MSC codes. 65M12, 65M15

1. Introduction.

In this paper we would like to present the L^2-norm stability analysis and obtain error estimate for the explicit single step time marching discontinuous Galerkin (ESTDG) method. Two well-known examples of this method include the RKDG method and the LWDG method, which respectively employ the Runge–Kutta time marching [5, 6, 7, 8, 9], and the Lax-Wendroff time marching [13, 22]. Many applications have shown that these methods are good at solving nonlinear conservation laws, due to good stability, high order accuracy and the ability for capturing shocks sharply. For more details, we refer to the review papers [10, 14, 19, 20] and the references therein.

Besides the time marching algorithms, the major concepts in these methods are the numerical fluxes in the DG spatial discretization. We remark that, in numerical applications, nonlinear limiters are also used to improve the numerical performance when shocks appear. However, in this paper we do not consider the limiters and only pay attention to the numerical fluxes. In most numerical experiments, numerical fluxes are often taken as the same type or with the same parameter at any element boundaries and any time stage. However, they are allowed to be changed and this strategy is also widely applied. A well-known example is the downwind treatment in high order RKDG methods to deal with the negative time marching coefficients [7, 10], which ensures the total variation diminishing in the means (TVDM) property (coupled

[1]School of Mathematical Sciences, Nanjing Normal University, Nanjing 210023, Jiangsu Province, China. E-mail: yuanxu@njnu.edu.cn. Research is partially supported by NSFC grant 12071214.

[2]Division of Applied Mathematics, Brown University, Providence, RI 02912, USA. E-mail: chi-wang_shu@brown.edu. Research is partially supported by NSF grant DMS-2010107.

[3]Department of Mathematics, Nanjing University, Nanjing 210093, Jiangsu Province, China. E-mail: qzh@nju.edu.cn. Research is partially supported by NSFC grant 12071214.

with a suitable limiter) under the strong-stability-preserving (SSP) framework [11] such that a good numerical performance might be obtained nearby the shock. This treatment is necessary because the Runge-Kutta algorithm for nonlinear problems must have negative time marching coefficients to achieve fifth or higher orders of time accuracy, or fourth order accuracy with only four stages [12, 16]. We would like to mention that the downwind treatment is also used in many high order numerical methods with, for instance, the Runge–Kutta algorithms [12, 15, 17, 21] and the multistep algorithms [18].

As far as the authors know, till now there is not any theoretical analysis of the ESTDG method with stage-dependent numerical flux functions, even for a simple model equation. To fill in this gap, we would like in this paper to consider the linear constant-coefficient hyperbolic equation in one dimension

$$\partial_t U + \beta \partial_x U = 0, \quad x \in I = (0,1), \quad t > 0, \tag{1.1}$$

which is equipped with the initial condition $U(x,0) = U_0(x)$. For simplicity, we take the periodic boundary condition and assume β to be a positive constant. In this paper, we will carry out the L^2-norm stability analysis and establish optimal error estimates of the ESTDG method in a unified framework. Different from the special case that numerical flux parameters are the same, we have to spend extra effort and propose a new strategy to carefully handle the analysis difficulties resulted from the perturbation of the numerical flux parameters.

There are two major difficulties to carry out the L^2-norm stability analysis. On one hand, it is well known [2] that the DG method coupled with the forward Euler time-marching is unstable for any fixed CFL number if the polynomial space is not piecewise constant. That is to say, the L^2-norm stability of ESTDG methods can not be derived under the SSP framework. We have to set up a facilitating energy equation to carry out the energy analysis. However, it is hardly accomplished for the high order in time fully discrete DG methods. Recently this trouble is systematically settled by the technique of matrix transferring process based on the temporal differences of stage solutions, which can automatically achieve the expected energy equation step by step. This technique has been successfully applied for the RKDG methods when numerical flux parameters are the same; see the references [1, 24, 25, 26, 27, 28]. On the other hand, in this paper we have to overcome the new difficulty resulting from the stage-dependent numerical flux parameters. As a main highlight of this paper, we make an extension and an application of the matrix transferring process and put forward an important quantity, named as *the averaged numerical flux parameter*. This quantity must be greater than one half and it reveals the overall upwind effect in every step time-marching. Further, we point out a strategy to enlarge this quantity by adjusting the numerical flux parameters, such that the stability performance of ESTDG methods can be improved from the strong stability to the monotonicity stability. For more detailed concepts and statements, see Section 3.

Unfortunately, for the ESTDG method with stage-dependent numerical flux parameters, the optimal error estimate becomes difficult, although the suboptimal error estimate is trivial by traditional treatments. If the numerical flux parameters are the same, this purpose has been achieved for the RKDG methods [25, 29, 30] by virtue of the above stability analysis and the generalized Gauss-Radau (GGR) projection with a fixed parameter. However, this proof strategy does not work well for the general case that numerical flux parameters are changed at different occurrence. The main reason is that the element boundary errors at different stages can not been simultaneously eliminated by a fixed GGR projection. To overcome this difficulty, we propose in this paper a new tool, named as *a series of space-time approximation functions* for a given spatial function. They preserve the local structure of the fully discrete scheme and the local balance of exact evolution under the rule of the considered differential equation. Hence, they are able to provide a group of good reference functions belonging to the finite element space, such that the error accumulation in time of the fully discrete scheme is elaborately scattered over the gap between the head function and the tail function (the first and the last one in this series). With the help of the results and the techniques proposed in the stability analysis, the difficulty to obtain the optimal error estimate is shifted to how to prove the optimal estimate to a series of space-time approximation functions. From our point of view, this analysis line is specifically designed for the fully discrete scheme and thus is remarkably distinguished to the traditional analysis line, which is used to start from the semi-discrete scheme in either time or space (in most literatures).

Because a series of space-time approximation functions are not regarded as the traditional projection, we are bound to encounter serious difficulties in proving the optimal approximation property; see Lemma 4.1. Fortunately, this aim can be accomplished by the aid of those techniques and concepts proposed in the matrix transferring process. Here we would like to emphasize that the averaged numerical flux parameter plays an important role in the entire analysis. To fully dig out the contribution of this quantity, we have to make a deep investigation on the matrix transferring process and make more efforts to establish the subtle relationship among the one-step time marching and the multistep one. This procedure involves many manipulations of matrices, including the Kronecker products of matrices. After some tedious and rigorous calculations, we discover a hidden zero restriction related to the averaged numerical flux parameter; see Proposition 4.1 or the equivalent identity (7.21). In fact, this hidden zero restriction is used almost everywhere in this paper. For example, it can help us to prove that the concerned submatrix in the multistep spatial matrix is close to a symmetric positive definite (SPD) matrix congruent to the Hilbert matrix such that the distance is reciprocal to the multistep number; see Lemma 3.4 and its proof in the appendix. Besides the above techniques, in this paper we also make use of the GGR projection and the flux lifting function (see Subsection 4.2) to complete the proof of Lemma 4.1.

The rest of paper is organized as follows. In Section 2 we describe the ESTDG method and then present two well-known examples. In Section 3 we present a framework to carry out the L^2-norm stability analysis, where the averaged numerical flux parameter is proposed. Section 4 is devoted to obtaining the optimal error estimate in L^2-norm, where a series of space-time approximation functions are proposed and analyzed. Some numerical experiments are given in Section 5 to verify the theoretical results. The concluding remarks and some technical proofs are respectively presented in Section 6 and the appendix.

2. The ESTDG method.

In this section we present the detailed definition of the ESTDG methods to solve the model equation (1.1) and show two well-known examples including the RKDG method and the LWDG method.

2.1. The semidiscrete DG method.

Let J be any positive integer and $0 = x_{1/2} < x_{3/2} < \cdots < x_{J-1/2} < x_{J+1/2} = 1$ be a quasi-uniform partition I_h of the spatial interval I. Each element $I_j = (x_{j-1/2}, x_{j+1/2})$ has the length $h_j = x_{j+1/2} - x_{j-1/2}$ for $j = 1, 2, \ldots, J$, and we denote $h = \max_{1\leq j\leq J} h_j$. Then we define the discontinuous finite element space by

$$V_h = \{\, v \in L^2(I) : v|_{I_j} \in \mathcal{P}^k(I_j),\ j = 1, 2, \ldots, J \,\}, \tag{2.1}$$

where $\mathcal{P}^k(I_j)$ is the polynomial space in I_j of degree at most $k \geq 0$. As usual we denote by v^+ and v^- the limits of v from two sides, and denote by

$$\{\!\{v\}\!\}^\theta = \theta v^- + (1-\theta)v^+, \quad [\![v]\!] = v^+ - v^-$$

the θ-weighted average and the jump at the element boundary, respectively.

The semidiscrete DG method to solve hyperbolic equation (1.1) is often defined as follows: find a map $u(t)\colon [0,T] \to V_h$ such that it satisfies

$$\Big(\partial_t u, v\Big)_{I_h} = \mathcal{H}^\theta(u,v), \quad \forall\, v \in V_h, \quad t \in (0,T], \tag{2.2}$$

with a well-defined initial solution $u(0) \in V_h$, where $\mathcal{H}^\theta(u,v)$ is the so-called spatial DG discretization in the form

$$\mathcal{H}^\theta(u,v) = \underbrace{\sum_{1\leq j\leq J} \int_{I_j} \beta u \partial_x v \mathrm{d}x}_{(\beta u, \partial_x v)_{I_h}} + \underbrace{\sum_{1\leq j\leq J} \beta \{\!\{u\}\!\}^\theta_{j+\frac12} [\![v]\!]_{j+\frac12}}_{\langle \beta \{\!\{u\}\!\}^\theta, [\![v]\!]\rangle_{\varGamma_h}}. \tag{2.3}$$

Here θ is called as the numerical flux parameter in this paper, and it is often assumed to be independent of time t and greater than $1/2$ in order to provide the upwind mechanism. In (2.3), the inner product in $L^2(I_h)$ and $L^2(\varGamma_h)$ are respectively denoted by $(\cdot,\cdot)_{I_h}$ and $\langle \cdot,\cdot\rangle_{\varGamma_h}$. The associated norms are $\|\cdot\|_{L^2(I)} = \|\cdot\|_{L^2(I_h)}$ and $\|\cdot\|_{L^2(\varGamma_h)}$, respectively. Here I_h is the partition and $\varGamma_h$ denotes all element boundaries.

The following properties [27] for the DG discretization (2.3) will be used. Let u and v be any functions in V_h below. A simple application of integration by parts yields the approximating skew-symmetric property

$$\mathcal{H}^\theta(u,v) + \mathcal{H}^\theta(v,u) = -\beta(2\theta-1)\Big\langle [\![u]\!], [\![v]\!] \Big\rangle_{\varGamma_h}, \tag{2.4a}$$

which implies the nonpositive property (if $\theta > 1/2$)

$$\mathcal{H}^\theta(u,u) = -\frac{1}{2}\beta(2\theta-1)\|[\![u]\!]\|^2_{L^2(\varGamma_h)}, \tag{2.4b}$$

to explicitly show the numerical viscosity in the spatial discretization. Moreover, we also have the weak boundedness property (with bounded parameter θ)

$$|\mathcal{H}^\theta(u,v)| \leq C\beta h^{-1}\|u\|_{L^2(I)}\|v\|_{L^2(I)}, \tag{2.4c}$$

where the bounding constant $C > 0$ depends on θ and the inverse constant μ in the following inequalities [4, 14]: for any $v \in V_h$ there hold

$$\|\partial_x v\|_{L^2(I)} \leq \mu h^{-1}\|v\|_{L^2(I)}, \quad \|v^\pm\|_{L^2(\varGamma_h)} \leq \mu h^{-\frac12}\|v\|_{L^2(I)}, \tag{2.5}$$

where $\mu > 0$ is independent of v and h.

2.2. The ESTDG methods. For simplicity, let $N>0$ be any positive integer and $\{t^n=n\tau\colon 0\le n\le N\}$ be a uniform partition of the time interval $[0,T]$, where $\tau=T/N$ is the time step. In this paper we would like to seek the numerical solution at time level t^n, denoted by $u^n\in V_h$, by employing an explicit single-step algorithm to solve the semidiscrete DG method (2.2).

Suppose that u^n has been obtained at the current time, we are able to seek u^{n+1} at the next time level through s intermediate (or generalized stage) solutions. The detailed procedure is often described in the Shu–Osher form as follows:

1. Let $u^{n,0}=u^n$.
2. For $\ell=0,1,\ldots,s-1$, successively find the generalized stage solution $u^{n,\ell+1}\in V_h$ through the variational formula

$$\left(u^{n,\ell+1},v\right)_{I_h}=\sum_{0\le\kappa\le\ell}\left[c_{\ell\kappa}\left(u^{n,\kappa},v\right)_{I_h}+\tau d_{\ell\kappa}\mathcal{H}^{\theta_{\ell\kappa}}(u^{n,\kappa},v)\right],\quad \forall\, v\in V_h. \tag{2.6}$$

   Here the time-marching parameters, $c_{\ell\kappa}$ and $d_{\ell\kappa}$, are inherited from the r-th order explicit single-step algorithm. In this paper we demand $d_{\ell\ell}\neq 0$ and $c_{\ell\kappa}\ge 0$ for any ℓ and κ. Note that $s\ge r$ in general.
3. Let $u^{n+1}=u^{n,s}$.

The initial solution $u^0\in V_h$ can be set as any approximation of U_0. In this paper we define it by the local L^2-projection $\mathbb{P}_h$, namely

$$\left(u^0,v\right)_{I_h}=\left(U_0,v\right)_{I_h},\quad \forall\, v\in V_h. \tag{2.7}$$

Till now we have completed the definition of the fully discrete method, which is named as the ESTDG(s,r,k) method in this paper for convenience.

We remark again that the numerical flux parameters in (2.6) are allowed to be changed at every stage. Compared with the special case that the numerical flux parameters are the same [27], the ESTDG methods provide a chance to improve the numerical performance by adjusting the numerical flux. To show that, we give two well-known examples in what follows.

Example 2.1. *Consider the RKDG$(4,4,k)$ method with the downwind treatment [21] to deal with the negative time-marching coefficients in*

$$\{c_{\ell\kappa}\}=\begin{pmatrix}1&&&\\1/2&1/2&&\\1/9&2/9&2/3&\\0&1/3&1/3&1/3\end{pmatrix},\quad \{d_{\ell\kappa}\}=\begin{pmatrix}1/2&&&\\-1/4&1/2&&\\-1/9&-1/3&1&\\0&1/6&0&1/6\end{pmatrix}, \tag{2.8}$$

where ℓ and κ are taken from $\{0,1,2,3\}$ in the natural order. To be more general, we would like in this paper to take the numerical flux parameters to be as follows: let $\theta_{\ell\kappa}>1/2$ if $d_{\ell\kappa}\ge 0$ and $\theta_{\ell\kappa}<1/2$ otherwise.

Example 2.2. *The LWDG(r,k) method adopts the rth order Lax–Wendroff time marching, which has been discussed in [13, 22] for $r\le 3$ with some special numerical flux parameters. More specifically, the original definition of the second order LWDG method [22] is given in the form*

$$\begin{aligned}\left(p^n,v\right)_{I_h}&=-\mathcal{H}^{\theta_{00}}(u^n,v),\\ \left(u^{n+1},v\right)_{I_h}&=\left(u^n,v\right)_{I_h}+\tau\mathcal{H}^{\theta_{10}}(u^n,v)-\frac{1}{2}\tau^2\mathcal{H}^{\theta_{11}}(p^n,v),\end{aligned} \tag{2.9}$$

where $\theta_{00} = \theta_{10} = 1$ and θ_{11} is 0 or 1. Here p is the approximation of the auxiliary variable $\beta\partial_x U$. Defining the stage solution $u^{n,1} = -\tau p^n$, we can write (2.9) into the ESTDG method.

Actually, the above statement is true for any r. Namely, the LWDG(r, k) method can be understood as an ESTDG(r, r, k) method with the contributory (or nonzero) parameters

$$c_{r-1,0} = 1; \quad d_{\ell\ell} = 1,\ 0 \le \ell \le r-2; \quad d_{r-1,\kappa} = \frac{1}{(\kappa+1)!},\ 0 \le \kappa \le r-1. \tag{2.10}$$

Due to the technical limitation, the numerical flux parameters are required to satisfy some conditions in [22], for example, $\theta_{00} = \theta_{r-1,0}$ sometimes. In this paper we would like to relax the above restrictions and investigate the generalized LWDG method.

3. Stability analysis.

In this section we will analyze the L^2-norm stability for the ESTDG methods. This analysis framework can be looked upon as an application and an extension of the technique of the matrix transferring process [27] when numerical flux parameters are the same.

3.1. The matrix transferring process.

In order to accurately understand the stability performance, we have to investigate the scheme for every multistep time-marching. For this purpose, we follow [25, 27] and introduce the generalized notations for stage solutions. Namely, for any nonnegative integers n, i and j, denote

$$u^{n,si+j} = u^{n+i,j}. \tag{3.1}$$

Remark that this notational rule has been used in the scheme's description.

Let $m \ge 1$ be a multistep number. It is evident for the ESTDG(s, r, k) method that every m-steps marching with time step τ can be regarded as one-step marching of an ESTDG(ms, r, k) method with time step $m\tau$. Namely, for $0 \le \ell \le ms-1$, the stage solutions satisfy the following variation formula: for any $v \in V_h$,

$$\Big(u^{n,\ell+1}, v\Big)_{I_h} = \sum_{0\le\kappa\le\ell} \Big[c_{\ell\kappa}(m)\Big(u^{n,\kappa}, v\Big)_{I_h} + m\tau d_{\ell\kappa}(m)\mathcal{H}^{\theta_{\ell\kappa}(m)}(u^{n,\kappa}, v)\Big]. \tag{3.2}$$

Let $\ell' = \ell \pmod s$ and $\kappa' = \kappa \pmod s$. The contributory parameters in (3.2) only emerge at those ℓ and κ satisfying $\ell - \ell' = \kappa - \kappa'$, such that

$$c_{\ell\kappa}(m) = c_{\ell'\kappa'}, \quad d_{\ell\kappa}(m) = \frac{1}{m} d_{\ell'\kappa'}, \quad \theta_{\ell\kappa}(m) = \theta_{\ell'\kappa'}. \tag{3.3}$$

Here ℓ' and κ' are both taken from $\{0, 1, \ldots, s-1\}$.

3.1.1. Temporal differences of stage solutions.

For $1 \le i \le ms$, we would like to follow [27, 25] and define the ith order temporal difference of stage solutions in the form

$$\mathbb{D}_i(m)u^n = \sum_{0\le j\le i} \sigma_{ij}(m)u^{n,j}, \tag{3.4}$$

where $\sigma_{ij}(m)$ are undetermined combination coefficients independent of stage solutions. For convenience, we denote $\mathbb{D}_0(m)u^n = u^n$ and $\sigma_{00}(m) = 1$ throughout this paper.

The combination coefficients in (3.4) can be inductively defined. Assuming the temporal differences of stage solutions up to the ith order have been well defined, we would like to write the next one $\mathbb{D}_{i+1}(m)u^n$ as a linear combination of the previous stage marching, independent of the spatial discretization, namely

$$\mathbb{D}_{i+1}(m)u^n = \sum_{0\le\ell\le i}\phi_{i\ell}(m)\Big[u^{n,\ell+1} - \sum_{0\le\kappa\le\ell}c_{\ell\kappa}(m)u^{n,\kappa}\Big], \tag{3.5}$$

where $\phi_{i\ell}(m)$ are combination coefficients given by the next procedure.

Let ϑ be any arbitrary fixed constant. Due to (3.2) and (3.5), after a changing of summation orders we yield

$$\Big(\mathbb{D}_{i+1}(m)u^n, v\Big)_{I_h} = m\tau\Phi_i(v) + m\tau\Psi_i(v), \tag{3.6}$$

where

$$\Phi_i(v) = \sum_{0\le\kappa\le i}\sum_{\kappa\le\ell\le i}\phi_{i\ell}(m)d_{\ell\kappa}(m)\mathcal{H}^{\vartheta}(u^{n,\kappa}, v), \tag{3.7a}$$

$$\Psi_i(v) = \sum_{0\le\kappa\le i}\sum_{\kappa\le\ell\le i}\phi_{i\ell}(m)d_{\ell\kappa}(m)\Big[\mathcal{H}^{\theta_{\ell\kappa}(m)}(u^{n,\kappa}, v) - \mathcal{H}^{\vartheta}(u^{n,\kappa}, v)\Big]. \tag{3.7b}$$

We first start from the main term (3.7a). Since every diagonal entry $d_{\kappa\kappa}(m)$ is nonzero, the triangular system of linear equations

$$\sum_{\kappa\le\ell\le i}\phi_{i\ell}(m)d_{\ell\kappa}(m) = \sigma_{i\kappa}(m), \quad \kappa = 0, 1, \dots, i \tag{3.8}$$

uniquely determines $\phi_{i\ell}(m)$ for $0 \le \ell \le i$. Substituting this into (3.7a), we can achieve the same expression as that in [25]

$$\Phi_i(v) = \mathcal{H}^{\vartheta}(\mathbb{D}_i(m)u^n, v). \tag{3.9}$$

At this moment, by (3.5) and (3.4) we are able to define

$$\sigma_{i+1,\kappa}(m) = \phi_{i,\kappa-1}(m) - \sum_{\kappa\le\ell\le i}\phi_{i,\ell}(m)c_{\ell\kappa}(m), \quad \kappa = 0, 1, \dots, i, \tag{3.10a}$$

with the supplemental notation $\phi_{i,-1}(m) = 0$, and

$$\sigma_{i+1,i+1}(m) = \phi_{ii}(m) = \frac{\sigma_{ii}(m)}{d_{ii}(m)} \neq 0. \tag{3.10b}$$

By these data we now get the definition of $\mathbb{D}_{i+1}(m)u^n$. Note that the above manipulations do not depend on the numerical flux parameters, hence the above $\sigma_{ij}(m)$ are the same as those in [25].

Next we turn to the perturbation term (3.7b), which is equal to zero if $\theta_{\ell\kappa} \equiv \vartheta$. We can uniquely determine $q_{i\ell}(m;\vartheta)$, for $0 \le \ell \le i$, by the triangular system of linear equations

$$\sum_{\kappa\le\ell\le i}q_{i\ell}(m;\vartheta)\sigma_{\ell\kappa}(m) = -\sum_{\kappa\le\ell\le i}\phi_{i\ell}(m)d_{\ell\kappa}(m)(\vartheta - \theta_{\ell\kappa}(m)), \quad \kappa = 0, 1, \dots, i, \tag{3.11}$$

because every diagonal entry is nonzero, due to (3.10b). Since a simple manipulation gives

$$\mathcal{H}^{\theta}(w, v) - \mathcal{H}^{\vartheta}(w, v) = \beta(\vartheta - \theta)\langle[\![w]\!], [\![v]\!]\rangle_{\Gamma_h},$$

by substituting (3.11) into (3.7b) and changing the summary order, we can deduce

$$
\begin{aligned}
\Psi_i(v) &= \beta \sum_{0\le\kappa\le i}\sum_{\kappa\le\ell\le i} \phi_{i\ell}(m) d_{\ell\kappa}(m)(\vartheta-\theta_{\ell\kappa}(m))\Big\langle [\![u^{n,\kappa}]\!], [\![v]\!]\Big\rangle_{\Gamma_h}\\
&= -\beta \sum_{0\le\kappa\le i}\sum_{\kappa\le\ell\le i} q_{i\ell}(m;\vartheta)\sigma_{\ell\kappa}(m)\Big\langle [\![u^{n,\kappa}]\!], [\![v]\!]\Big\rangle_{\Gamma_h}\\
&= -\beta \sum_{0\le\ell\le i} q_{i\ell}(m;\vartheta)\Big\langle [\![\mathbb{D}_\ell(m)u^n]\!], [\![v]\!]\Big\rangle_{\Gamma_h},
\end{aligned}
\tag{3.12}
$$

where (3.4) is used also at the last step. Substituting (3.9) and (3.12) into (3.6), we eventually achieve the relationship among the temporal differences of stage solutions: for any $v\in V_h$, there holds

$$
\Big(\mathbb{D}_{i+1}(m)u^n, v\Big)_{I_h} = m\tau\mathcal{H}^\vartheta(\mathbb{D}_i(m)u^n, v) - m\tau\beta\sum_{0\le\ell\le i} q_{i\ell}(m;\vartheta)\Big\langle [\![\mathbb{D}_\ell(m)u^n]\!], [\![v]\!]\Big\rangle_{\Gamma_h}.
\tag{3.13}
$$

This formula obviously degenerates to that in [27] if $\theta_{\ell\kappa}\equiv\vartheta$, since $q_{i\ell}(m;\vartheta)=0$ now.

It is worthy to mention again that the right hand side of (3.13) is independent of the choice of ϑ. To show that, we would like to denote

$$
\tilde{q}_{i\ell}(m;\vartheta) = q_{i\ell}(m;\vartheta) + \delta_{i\ell}\vartheta,
\tag{3.14}
$$

where $\delta_{i\ell}$ is a Kronecker symbol, being 1 if $i=\ell$ and otherwise 0. In fact, these quantities satisfy the triangular system of linear equations

$$
\sum_{\kappa\le\ell\le i}\tilde{q}_{i\ell}(m;\vartheta)\sigma_{\ell\kappa}(m) = \sum_{\kappa\le\ell\le i}\phi_{i\ell}(m)d_{\ell\kappa}(m)\theta_{\ell\kappa}(m), \quad \kappa=0,1,\dots i,
$$

due to (3.11) and (3.8). Hence $\tilde{q}_{i\ell}(m;\vartheta)$ is independent of ϑ and is therefore denoted by $\tilde{q}_{i\ell}(m)$ in this paper. With this notation, we can write (3.13) into an equivalent form

$$
\Big(\mathbb{D}_{i+1}(m)u^n, v\Big)_{I_h} = m\tau\mathcal{H}^0(\mathbb{D}_i(m)u^n, v) - m\tau\beta\sum_{0\le\ell\le i} \tilde{q}_{i\ell}(m)\Big\langle [\![\mathbb{D}_\ell(m)u^n]\!], [\![v]\!]\Big\rangle_{\Gamma_h},
\tag{3.15}
$$

which shows its independence of ϑ.

3.1.2. Derivation of energy equations. After all the temporal differences of stage solutions have been defined by (3.4), the inversion manipulation yields the linear equivalence of two function sequences $\{u^{n,0}, u^{n,1},\dots,u^{n,ms}\}$ and $\{\mathbb{D}_0(m)u^n, \mathbb{D}_1(m)u^n, \dots, \mathbb{D}_{ms}(m)u^n\}$. Specially, there holds the evolution identity

$$
u^{n+m} = \sum_{0\le i\le ms}\alpha_i(m)\mathbb{D}_i(m)u^n,
\tag{3.16}
$$

where the evolution coefficient $\alpha_i(m)$ only depends on the time-marching coefficients, $c_{\ell\kappa}$ and $d_{\ell\kappa}$. The detailed relationship will be discussed in the appendix.

REMARK 3.1. *In [25, 27], we have written* (3.16) *in the form*

$$
\alpha_0(m)u^{n+m} = \sum_{0\le i\le ms}\alpha_i(m)\mathbb{D}_i(m)u^n,
$$

where $\alpha_0(m)>0$ is introduced only for scaling. In this paper we always take $\alpha_0(m)=1$ for convenience.

It is proved in [24, Lemma 2.2] that

$$\alpha_\ell(m) = 1/\ell!, \quad 0 \le \ell \le r, \tag{3.17}$$

which will be frequently used, especially for $\ell = 0, 1$.

Along the same line as that in the previous works [24, 27], we can carry out the matrix transferring process to automatically achieve a perfect energy equation for the considered ESTDG method, through a sequence of energy equations

$$\|u^{n+m}\|^2_{L^2(I)} - \|u^n\|^2_{L^2(I)} = \mathrm{TM}(\ell;m) + \mathrm{SP}(\ell;m). \tag{3.18}$$

Here $\ell \ge 0$ stands for the sequence number, and

$$\mathrm{TM}(\ell;m) = \sum_{0\le i\le ms}\sum_{0\le j\le ms} a^{(\ell)}_{ij}(m)\Big(\mathbb{D}_i(m)u^n, \mathbb{D}_j(m)u^n\Big)_{I_h}, \tag{3.19a}$$

$$\mathrm{SP}(\ell;m) = -m\tau\beta\sum_{0\le i\le ms}\sum_{0\le j\le ms} b^{(\ell)}_{ij}(m)\Big\langle [\![\mathbb{D}_i(m)u^n]\!], [\![\mathbb{D}_j(m)u^n]\!]\Big\rangle_{\Gamma_h}, \tag{3.19b}$$

respectively express the temporal information and spatial information. For convenience, we abbreviate (3.19) by two symmetric matrices

$$\mathbb{A}^{(\ell)}(m) = \{a^{(\ell)}_{ij}(m)\}_{0\le i,j\le ms}, \quad \mathbb{B}^{(\ell)}(m) = \{b^{(\ell)}_{ij}(m)\}_{0\le i,j\le ms}. \tag{3.20}$$

For $\ell = 0$, the initial energy equation can be derived from the evolution identity (3.16) by squaring and integrating. It deduces the initial matrices with

$$a^{(0)}_{ij}(m) = \begin{cases} 0, & i=j=0,\\ \alpha_i(m)\alpha_j(m), & \text{otherwise}; \end{cases} \quad \text{and } b^{(0)}_{ij}(m) = 0. \tag{3.21}$$

This energy equation does not reflect any contribution of the spatial discretization. For this reason, we transfer the temporal information into the spatial information step by step, in order to look for more contribution of the spatial information in each step. In this process, the major object is the joint of two temporal information terms

$$\mathcal{J}(i,j) = \Big(\mathbb{D}_{i+1}(m)u^n, \mathbb{D}_j(m)u^n\Big)_{I_h} + \Big(\mathbb{D}_i(m)u^n, \mathbb{D}_{j+1}(m)u^n\Big)_{I_h}, \tag{3.22}$$

which satisfies the following lemma.

Lemma 3.1. *For $0 \le i, j \le ms-1$, there holds*

$$\mathcal{J}(i,j) = -m\tau\beta\Big[-\mathcal{P}(i,j) + \sum_{0\le i'\le i}\tilde{q}_{ii'}(m)\mathcal{P}(i',j) + \sum_{0\le j'\le j}\tilde{q}_{jj'}(m)\mathcal{P}(i,j')\Big], \tag{3.23}$$

where $\mathcal{P}(i',j') = \langle [\![\mathbb{D}_{i'}(m)u^n]\!], [\![\mathbb{D}_{j'}(m)u^n]\!]\rangle_{\Gamma_h}$ is the essential ingredient of the spatial information.

Proof. This lemma follows from (3.15) and (2.4a). ∎

Remark 3.2. *For $\theta_{\ell\kappa} \equiv \theta$, it is easy to see $q_{\ell\kappa}(m;\theta) = 0$ and*

$$\mathcal{J}(i,j) = -m\tau\beta(2\theta-1)\mathcal{P}(i,j),$$

from the above lemma. This result is the same as that in [27].

Below we are going to describe the detailed transform in each step. By induction, assume for $\ell \geq 1$ that we have obtained two matrices

$$\mathbb{A}^{(\ell-1)} = \left(\begin{array}{c:c:c c} \mathbb{O} & \mathbb{O} & \mathbb{O} & \cdots \\ \hdashline \mathbb{O} & a^{(\ell-1)}_{\ell-1,\ell-1} & a^{(\ell-1)}_{\ell-1,\ell} & \cdots \\ \hdashline \mathbb{O} & a^{(\ell-1)}_{\ell,\ell-1} & a^{(\ell-1)}_{\ell-1,\ell-1} & \cdots \\ \vdots & \vdots & \vdots & \ddots \end{array}\right), \quad \mathbb{B}^{(\ell-1)} = \left(\begin{array}{c:c:c c} \star & \star & \star & \cdots \\ \hdashline \star & b^{(\ell-1)}_{\ell-1,\ell-1} & b^{(\ell-1)}_{\ell-1,\ell} & \cdots \\ \hdashline \star & b^{(\ell-1)}_{\ell,\ell-1} & 0 & \cdots \\ \vdots & \vdots & \vdots & \ddots \end{array}\right),$$

where $\mathbb{O}$ remarks the zero block and $\star$ remarks the transformed (nonzero) region. Here and below (m) is dropped for convenience unless otherwise stated.

The next action depends on the leading element $a^{(\ell-1)}_{\ell-1,\ell-1}$ in the temporal matrix. If it is equal to zero, we carry out the ℓ-th step transform. Associated with the temporal matrix $\mathbb{A}^{(\ell-1)}(m)$, we successively eliminate every entry at the $(\ell-1)$-th row and column by transforming the related joint of temporal information (i.e., those entries at the ℓ-th row and column) into spatial information. This purpose can be achieved by an application of Lemma 3.1.

More specifically, the new temporal matrix is denoted by $\mathbb{A}^{(\ell)}(m)$, whose entries at the lower triangular region are defined as

$$a^{(\ell)}_{ij} = \begin{cases} 0, & \ell-1 \leq i \leq ms \text{ and } j = \ell-1, \\ a^{(\ell-1)}_{ij} - 2a^{(\ell-1)}_{i+1,j-1}, & i = \ell \text{ and } j = \ell, \\ a^{(\ell-1)}_{ij} - a^{(\ell-1)}_{i+1,j-1}, & \ell+1 \leq i \leq ms-1 \text{ and } j = \ell, \\ a^{(\ell-1)}_{ij}, & \text{otherwise.} \end{cases} \tag{3.24}$$

Since $\mathbb{A}^{(\ell)}(m)$ is symmetric, the upper triangular entry is easily filled in. We remark that the only difference between the second line and the third line results from whether the basic elimination (with respect to one entry) along the row and column is superimposed on the same position.

The above operation is accompanied by the changing of the spatial matrix. For each basic elimination, the modified entries spread over at one row and column, due to Lemma 3.1. As a result, it is hard to present a short unified formulas for calculating each entry of $\mathbb{B}^{(\ell)}(m)$. However, this manipulation process can be conveniently expressed in the pseudo-code and summarized as **Algorithm** 1.

Algorithm 1. Generate the spatial matrix $\mathbb{B}^{(\ell)} = \{b^{(\ell)}_{ij}\}$ for the given ℓ.

Step 1. Initialization: set $g_{ij} = 0$ for any $0 \leq i, j \leq ms$;

Step 2. Modification: for $\kappa = \ell-1, \ldots, ms-1$, do

if $\kappa = \ell-1$ then let $\nu = 1/2$; otherwise, $\nu = 1$;

compute $g_{\kappa,\ell-1} \leftarrow g_{\kappa,\ell-1} - \nu a^{(\ell-1)}_{\kappa+1,\ell-1}$;

compute $g_{i,\ell-1} \leftarrow g_{i,\ell-1} + \nu a^{(\ell-1)}_{\kappa+1,\ell-1}\tilde{q}_{\kappa,i}$ for $i = 0, \ldots, \kappa$;

compute $g_{\kappa,j} \leftarrow g_{\kappa,j} + \nu a^{(\ell-1)}_{\kappa+1,\ell-1}\tilde{q}_{\ell-1,j}$ for $j = 0, \ldots, \ell-1$;

Step 3. Generation: define $b^{(\ell)}_{ij} = b^{(\ell-1)}_{ij} + g_{ij} + g_{ji}$ for $0 \leq i, j \leq ms$.

Otherwise, if $a^{(\ell-1)}_{\ell-1,\ell-1}$ is not equal to zero, we stop the entire transform process and name this entry as the *central objective*. At the same time, we output the *termination* *index* of time marching

$$\zeta(m) = \ell - 1, \tag{3.25}$$

as well as the ultimate temporal matrix $\mathbb{A}(m) = \mathbb{A}^{(\zeta(m))}(m)$ and the ultimate spatial matrix $\mathbb{B}(m) = \mathbb{B}^{(\zeta(m))}(m)$.

Till now we have completed the description of the matrix transferring process.

3.1.3. Some important quantities. Since the ultimate temporal matrix $\mathbb{A}(m)$ solely depends on the time marching coefficients, we have the same conclusions as those in [24].

LEMMA 3.2. *For $m \geq 1$, the termination index of time marching satisfies $\zeta(m) = \zeta$, and moreover, the central objective $a_{\zeta\zeta}(m)$ preserves the sign.*

The ultimate spatial matrix $\mathbb{B}(m)$ depends on not only the time marching but also the numerical flux parameters. Motivated by the previous work [27], it is also important to find the largest order of the sequential principal submatrix to be SPD. In this paper, this quantity

$$\rho(m) = \max\Big\{\kappa\colon 1 \leq \kappa \leq \zeta \text{ and } \{b_{ij}(m)\}_{0\leq i,j\leq \kappa-1} \text{ is SPD}\Big\} \tag{3.26}$$

is also named as the *contribution index* of the spatial discretization. If $b_{00}(m) \leq 0$, we define $\rho(m) = 0$ as a supplement.

From the practical viewpoint, we would like in this paper to assume we always have $\rho(m) \geq 1$. This assumption is equivalent to that the averaged numerical flux parameter for every m-step time marching

$$\Theta(m) \equiv \frac{1}{2}\Big[b_{00}(m) + 1\Big] \tag{3.27}$$

is always greater than $1/2$. From **Algorithm 1**, it is easy to see that

$$b_{00}(m) \equiv b_{00}^{(1)}(m) = -a_{10}^{(0)}(m) + \sum_{0\leq \ell\leq ms-1} 2a_{\ell+1,0}^{(0)}(m)\tilde{q}_{\ell,0}(m),$$

which is determined at the first step of the matrix transferring process. Noticing (3.21) and $\alpha_1(m) = 1$, it follows from (3.27) that

$$\Theta(m) = \sum_{0\leq \ell\leq ms-1} \alpha_{\ell+1}(m)\tilde{q}_{\ell,0}(m). \tag{3.28}$$

If all the numerical flux parameters are the same, i.e., $\theta_{\ell\kappa} = \theta$, it is easy to get $\Theta(m) = \theta$ for all $m \geq 1$. Actually, this property for the special case can be generalized to variant numerical flux parameters.

LEMMA 3.3. *$\Theta(m)$ is independent of m, and is therefore denoted by Θ in this paper.*

We postpone the proof of this lemma to the appendix, since it shares many materials in the proof of the next lemma.

LEMMA 3.4. *If $\Theta > 1/2$, then there exists an $m_\star \geq 1$ such that $\rho(m) = \zeta$ for $m \geq m_\star$.*

The proof line is the same as that for the special case that the numerical flux parameters are fixed [24]. However, the detailed process involves many matrix manipulation and looks more lengthy and technical. Hence we also postpone the proof of this lemma to the appendix.

Owing to Lemma 3.3, we name Θ as *the averaged numerical flux parameter* of the ESTDG method. We think that this quantity gives a more accurate description on the numerical viscosity for the fully discrete method. We would like to mention again that the assumption throughout this paper

$$\Theta > 1/2$$

means the upwind mechanism, at least in the average sense. This assumption will play an important role in the whole analysis of this paper.

In terms of the commonly accepted concept that the greater numerical viscosity ensures the better stability performance, we want to enlarge Θ to improve the stability performance of the ESTDG methods. This can be implemented by using the following two propositions, whose proofs will be given in the appendix.

PROPOSITION 3.1. *As a linear function of the numerical flux parameters, Θ is monotonically increasing with respect to $\theta_{\ell\kappa}$ if $d_{\ell\kappa} > 0$ and monotonically decreasing otherwise.*

For the RKDG method, the averaged numerical flux parameter often depends on every numerical flux parameter. For example, the RKDG$(4, 4, k)$ method (2.8) has

$$\Theta = \frac{37}{108}\theta_{00} - \frac{5}{36}\theta_{10} + \frac{5}{18}\theta_{11} - \frac{1}{27}\theta_{20} - \frac{1}{9}\theta_{21} + \frac{1}{3}\theta_{22} + \frac{1}{6}\theta_{31} + \frac{1}{6}\theta_{33}.$$

However, it is a little different for the LWDG method.

PROPOSITION 3.2. *For the LWDG(r, k) method we always have $\Theta = \theta_{r-1,0}$.*

Together with $\Theta > 1/2$, Proposition 3.2 gives a theoretical support to the upwind requirement $\theta_{r-1,0} > 1/2$ for the LWDG method, which has been implicitly stressed in [13, 22]. This proposition also shows that only this term must be discretized with the upwind mechanism, and the other terms can be arbitrarily done.

3.2. Energy analysis and main conclusions. By the matrix transferring process, we obtain the final energy equation (3.18) with $\ell = \zeta$, as well as the central objective and the contribution index of the spatial discretization. By the energy analysis, we are able to conclude the L^2-norm stability performance along the same line as that in [27].

The stage-dependent numerical flux parameters do not cause any essential difficulty in the stability analysis, since the increment every m steps is still bounded in the form

$$\|u^{n+m}\|^2_{L^2(I)} - \|u^n\|^2_{L^2(I)} \le a^{(\zeta)}_{\zeta\zeta}(m)\|\mathbb{D}_\zeta(m)u^n\|^2_{L^2(I)} + \Delta_1 + \Delta_2 + \Delta_3, \tag{3.29}$$

where

$$\begin{aligned}
\Delta_1 &= -\varepsilon_\star(m)m\tau\beta \sum_{0\le\ell<\rho(m)} \|[\![\mathbb{D}_\ell(m)u^n]\!]\|^2_{L^2(\Gamma_h)},\\
\Delta_2 &= C(m) \sum_{i,j\ge\zeta \text{ except } i=j=\zeta} \left|\Big(\mathbb{D}_i(m)u^n, \mathbb{D}_j(m)u^n\Big)_{I_h}\right|,\\
\Delta_3 &= C(m) \sum_{\max(i,j)\ge\rho(m)} \tau\left|\Big\langle [\![\mathbb{D}_i(m)u^n]\!], [\![\mathbb{D}_j(m)u^n]\!]\Big\rangle_{\Gamma_h}\right|,
\end{aligned}$$

with $\varepsilon_\star(m)$ being the smallest eigenvalue of the SPD submatrix $\{b_{ij}(m)\}_{0\le i,j\le \rho(m)-1}$. All terms in Δ_2 and Δ_3 (using the inverse inequality) can be easily controlled by the relationship

$$\|\mathbb{D}_{i+1}(m)u^n\|_{L^2(I)} \le C\lambda\|\mathbb{D}_i(m)u^n\|_{L^2(I)} + C(\tau\beta\lambda)^{\frac12}\sum_{0\le\ell\le i}\|[\![\mathbb{D}_\ell(m)u^n]\!]\|_{L^2(\mathit{\Gamma}_h)},$$

which is gotten by taking $v=\mathbb{D}_{i+1}(m)u^n$ in (3.13) and using (2.4c). Here $\lambda=|\beta|\tau/h$ is the CFL number and the last sum on the right hand side originates from the perturbation of the numerical flux parameters. This sum causes the only difference that we must encounter some terms involved the jumps of lower order temporal differences in order to bound each term in Δ_2 and Δ_3; however, they are still well controlled with the help of Δ_1. Hence the final stability results are the same just like before, if they are not specified for the detailed scheme. We would like to assert them without proofs, in order to shorten the length of this paper.

The next theorem is easily obtained by Lemma 3.4 and the rough estimate

$$\|u^{n+m}\|^2_{L^2(I)} \le \Big[1+C\lambda^{\min(2\zeta,2\rho(m)+1)}\Big]\|u^n\|^2_{L^2(I)},$$

due to the above two inequalities together with the inverse inequality. This result does not consider the effect of the sign of the central objective.

THEOREM 3.1. *The ESTDG method* (2.6) *has the weak(2ζ) stability. Namely, for sufficiently small h, there holds*

$$\|u^n\|_{L^2(I)} \le C\|u^0\|_{L^2(I)}, \quad n\ge 0, \tag{3.30}$$

under a stronger temporal-spatial condition $\tau \le Mh^{\frac{2\zeta}{2\zeta-1}}$ for sufficiently small h. Here M is any given positive constant, and the bounding constant $C=C(T,M)$ is independent of n,h and τ.

We would like to pay more attention on the stability results under suitable CFL conditions. To do that, we introduce an important quantity

$$n_\star = \min\Big\{m\colon \rho(m)=\rho(m+1)=\cdots=\rho(2m-1)=\zeta\Big\}, \tag{3.31}$$

which satisfies $n_\star \le m_\star$ due to Lemma 3.4. Note that the negative central objective plays a pivotal role in the next theorem.

THEOREM 3.2. *If the central objective keeps negative, the method* (2.6) *has the strong($n_\star$) stability for $k\ge 0$, namely, there exists a maximal CFL number $\lambda_{\max}>0$ such that*

$$\|u^n\|_{L^2(I)} \le \|u^0\|_{L^2(I)}, \quad n\ge n_\star, \tag{3.32}$$

holds under the CFL condition $\lambda\le\lambda_{\max}$. Furthermore, if $n_\star=1$ is allowed, the method actually has the monotonicity stability, since

$$\|u^{n+1}\|_{L^2(I)} \le \|u^n\|_{L^2(I)}, \quad n\ge 0. \tag{3.33}$$

Along the same line as that in [24, 27], we can similarly obtain a nice control among the temporal differences of stage solutions, for instance

$$\|\mathbb{D}_{i+1}(m)u^n\|_{L^2(I)} \le C\|(m\tau\beta\partial_x)\mathbb{D}_i(m)u^n\|_{L^2(I)} + C(\tau\beta\lambda)^{\frac12}\sum_{0\le\ell\le i}\|[\![\mathbb{D}_\ell(m)u^n]\!]\|_{L^2(\mathit{\Gamma}_h)}.$$

The derivative operation on the right hand side helps us to enhance the stability performance for piecewise polynomials of lower degree. The related conclusions are stated in the next theorem.

THEOREM 3.3. *The method* (2.6) *has the strong($n_\star$) stability for $k < \zeta$, if the central objective keeps positive. The method has the monotonicity stability for $k < \rho(1)$ no matter whether the central objective is positive or negative.*

From the last two theorems we are happy to find out an opportunity to enlarge the contribution index of spatial discretization so that the strong stability is improved to the monotonicity stability, by means of suitably adjusting the numerical flux parameters. In the next subsections we give some examples to show that.

3.2.1. The RKDG method. Consider the RKDG$(4,4,k)$ method proposed in Example 2.1. As an example, the numerical flux parameters are defined as

$$\left\{\theta_{\ell\kappa} - \frac{1}{2}\right\} = \varepsilon \begin{pmatrix} 1 & & & \\ -1 & 1 & & \\ -1 & -y & 1 & \\ & 1 & & 1 \end{pmatrix}, \tag{3.34}$$

where ε and y are two positive constants. Three negative entries in the right matrix correspond to the so-called downwind treatment.

We begin the stability analysis with $m = 1$. The temporal differences of stage solutions are defined as

$$\{\sigma_{ij}(1)\} = \begin{pmatrix} 1 & & & & \\ -2 & 2 & & & \\ 0 & -4 & 4 & & \\ 4 & 0 & -8 & 4 & \\ 8 & 0 & -16 & -16 & 24 \end{pmatrix}, \quad 0 \le i, j \le 4,$$

and the numerical flux parameters lead to

$$\left\{\tilde{q}_{ij}(1) - \frac{1}{2}\delta_{ij}\right\} = \varepsilon \begin{pmatrix} 1 & & & \\ 2 & 1 & & \\ -4/9 + 4y/3 & 2/3 + 2y/3 & 1 & \\ -100/9 - 8y/3 & -4/3 - 4y/3 & 0 & 1 \end{pmatrix}, \quad 0 \le i, j \le 3.$$

The matrix transferring process gives two matrices. The first one is the ultimate temporal matrix

$$\mathbb{A}(1) = \begin{pmatrix} \mathbb{O}_3 & & \\ & -1/72 & 1/144 \\ & 1/144 & 1/576 \end{pmatrix},$$

where $\mathbb{O}_3$ is third order zero matrix. This matrix implies that the termination index of time marching is $\zeta = 3$ and the central objective satisfies $a_{\zeta\zeta}(1) = -1/72 < 0$. The second one is the ultimate spatial matrix

$$\mathbb{B}(1) = \varepsilon \begin{pmatrix} 2y/9+79/27 & y/9+65/54 & 1/3 & y/36+17/108 & 0 \\ y/9+65/54 & y/18+13/18 & 1/4 & y/72+7/72 & 0 \\ 1/3 & 1/4 & 1/12 & 1/24 & 0 \\ y/36+17/108 & y/72+7/72 & 1/24 & 0 & 0 \\ 0 & 0 & 0 & 0 & 0 \end{pmatrix},$$

of which the first three leading principle determinants are

$$\varepsilon\Big(\frac{2y}{9}+\frac{79}{27}\Big), \quad \varepsilon^2\Big(\frac{y}{18}+\frac{1937}{2916}\Big), \quad \varepsilon^3\Big(\frac{y}{324}-\frac{125}{17496}\Big). \tag{3.35}$$

For $y > 125/54$, these three quantities are all positive and hence $\rho(1) = 3 = \zeta$. Now we can claim the monotonicity stability for $k \geq 0$ by Theorem 3.2.

For $y < 125/54$, the stability performance becomes weaker. To show that, we take $y = 1$ as an example and thus θ_{21} becomes bigger. From the first quantity in (3.35), we know that the averaged numerical flux parameter indeed satisfies Proposition 3.1. In this case, only the first two quantities in (3.35) are positive, and thus $\rho(1) = 2$ becomes smaller as we have predicted in the theory. A series of matrix transform process for multisteps time-marching yields $\rho(2) = \rho(3) = 3 = \zeta$. By Theorems 3.2 and 3.3 we can claim the strong(2) stability for any $k \geq 0$ and can not claim the monotonicity stability for $k \geq 2$. This statement looks a little weaker than the previous case, however, its sharpness will be shown in the numerical experiments.

3.2.2. The LWDG method. We now turn to the LWDG(r,k) method with $r \leq 5$; see Example 2.2. For simplicity, numerical flux parameters are taken to be $1/2 \pm \varepsilon$, where ε is a positive constant. Due to Proposition 3.2, we must set $\theta_{r-1,0} = 1/2+\varepsilon$ for all cases.

Take the second order ($r = 2$) LWDG method as an example. By the matrix transferring process we can obtain

$$\{\sigma_{ij}(1)\}_{0\leq i,j\leq 2} = \begin{pmatrix} 1 & & \\ 0 & 1 & \\ -2 & -2 & 2 \end{pmatrix} \quad \text{and} \quad \mathbb{A}(1) = \begin{pmatrix} 0 & & \\ & 0 & \\ & & 1/4 \end{pmatrix},$$

and get $\zeta = 2$ and $a_{\zeta\zeta}(1) = 1/4$. Due to Theorem 3.1, we claim that this method has at least the weak(4) stability for $k \geq 0$.

Due to Theorem 3.3, we can get the strong stability for lower degree k. For every combination of θ_{00} and θ_{11}, we may achieve different value of $n_\star$ by calculating the contribution index of spatial discretization as m increases. The detailed conclusions are listed as follows.

- Let $\theta_{00} = \theta_{11} = 1/2+\varepsilon$. We get $\rho(1) = 2 = \zeta$, since

$$\{\tilde{q}_{ij}(1)\}_{0\leq i,j\leq 1} = \begin{pmatrix} 1/2+\varepsilon & \\ & 1/2+\varepsilon \end{pmatrix}, \quad \{b_{ij}(1)\}_{0\leq i,j\leq 1} = \varepsilon \begin{pmatrix} 2 & 1 \\ 1 & 1 \end{pmatrix}.$$

Hence we conclude the monotonicity stability for $k \leq 1$.

- Let $\theta_{00} = 1/2 + \varepsilon$ and $\theta_{11} = 1/2 - \varepsilon$. Let $m = 1$ and we get

$$\{\tilde{q}_{ij}(1)\}_{0\le i,j\le 1} = \begin{pmatrix} 1/2+\varepsilon & \\ & 1/2-\varepsilon \end{pmatrix}, \quad \{b_{ij}(1)\}_{0\le i,j\le 1} = \varepsilon \begin{pmatrix} 2 & 0 \\ 0 & -1 \end{pmatrix},$$

  which implies $\rho(1) = 1$ and hence the monotonicity stability for $k = 0$. By carrying out the matrix transferring process for increasing multistep, we have $\rho(3) = \rho(4) = \rho(5) = 2 = \zeta$ and then conclude the strong(3) stability for $k \le 1$.
- The other cases can be studied similarly.

The stability results for the LWDG$(2, k)$ method are gathered in Table 3.1, where $\pm$ stands for $1/2 \pm \varepsilon$ here and below.

TABLE 3.1
Stability results for the LWDG$(2, k)$ methods.

parameters				$n_\star$: strong$(n_\star)$ stability	
θ_{00}	θ_{10}	θ_{11}	$k \ge 2$	$k = 1$	$k = 0$
+	+	+	weak(4)	1	1
+	+	−		3	
−	+	+		3	
−	+	−		4	

For $r = 3$ and 4, we are able to similarly find $\zeta = r - 1$ and the central objective is negative. Hence we can claim the strong stability for $k \ge 0$, due to Theorem 3.2. The detailed results are collected in Tables 3.2 and 3.3.

TABLE 3.2
Stability conclusions for the LWDG$(3, k)$ method.

parameters					$n_\star$: strong$(n_\star)$ stability	
θ_{00}	θ_{11}	θ_{20}	θ_{21}	θ_{22}	$k \ge 1$	$k = 0$
+	±	+	+	±	1	1
+	−	+	−	±	3	
−	−	+	±	±	3	
+	+	+	−	±	4	
−	+	+	±	±	4	

For $r = 5$, we get $\zeta = 3$ and the central objective is positive, which implies the strong stability for $k \le 2$ due to Theorem 3.3 and the weak(6) stability for $k \ge 3$ due to Theorem 3.1. The detailed results are collected in Table 3.4.

REMARK 3.3. *In the above four tables, the first row gives the numerical flux parameters to ensure the monotonicity stability for some k. For $r \ne 4$, it is acceptable to take $\theta_{\ell\kappa} \equiv 1/2 + \varepsilon$ for any ℓ and κ. However, for $r = 4$, we have to take $\theta_{22} = 1/2 - \varepsilon$ and take the others to be $\theta_{\ell\kappa} \equiv 1/2 + \varepsilon$.*

REMARK 3.4. *The LWDG$(2, 1)$ method with $\theta_{00} = \theta_{10} = 1$ and $\theta_{11} = 0$ (taking the second row in Table 3.1 with $\varepsilon = 1/2$) has been studied in [22], where the authors*

TABLE 3.3
Stability conclusions for the LWDG$(4, k)$ method.

parameters							$n_\star$: strong($n_\star$) stability		
θ_{00}	θ_{11}	θ_{22}	θ_{30}	θ_{31}	θ_{32}	θ_{33}	$k \geq 2$	$k = 1$	$k = 0$
$+$	$+$	$-$	$+$	$+$	$+$	$\pm$	1	1	
$+$	$\pm$	$+$	$+$	$+$	$+$	$\pm$	2	1	
$+$	$-$	$-$	$+$	$+$	$\pm$	$\pm$	2	1	
$+$	$+$	$\pm$	$+$	$+$	$-$	$\pm$	3	1	
$+$	$-$	$+$	$+$	$+$	$-$	$\pm$	3	1	
$+$	$-$	$\pm$	$+$	$-$	$+$	$\pm$	5	3	1
$+$	$-$	$\pm$	$+$	$-$	$-$	$\pm$	6	3	
$-$	$-$	$\pm$	$+$	$+$	$\pm$	$\pm$	6	3	
$-$	$-$	$\pm$	$+$	$-$	$\pm$	$\pm$	7	3	
$+$	$+$	$\pm$	$+$	$-$	$\pm$	$\pm$	7	3	
$-$	$+$	$\pm$	$+$	$+$	$\pm$	$\pm$	7	3	
$-$	$+$	$\pm$	$+$	$-$	$\pm$	$\pm$	8	4	

TABLE 3.4
Stability results for the LWDG$(5, k)$ method.

parameters										$n_\star$: strong($n_\star$) stability		
θ_{00}	θ_{11}	θ_{22}	θ_{33}	θ_{40}	θ_{41}	θ_{42}	θ_{43}	θ_{44}	$k \geq 3$	$k = 2$	$k = 1$	$k = 0$
$+$	$+$	$\pm$	$\pm$	$+$	$+$	$+$	$\pm$	$\pm$		1	1	
$+$	$-$	$-$	$\pm$	$+$	$+$	$\pm$	$\pm$	$\pm$		2	1	
$+$	$-$	$+$	$\pm$	$+$	$+$	$+$	$\pm$	$\pm$		2	1	
$+$	$-$	$+$	$\pm$	$+$	$+$	$-$	$\pm$	$\pm$		3	1	
$+$	$+$	$\pm$	$\pm$	$+$	$+$	$-$	$\pm$	$\pm$		3	1	
$+$	$-$	$\pm$	$\pm$	$+$	$-$	$+$	$\pm$	$\pm$	weak(6)	5	3	1
$+$	$-$	$\pm$	$\pm$	$+$	$-$	$-$	$\pm$	$\pm$		6	3	
$-$	$-$	$\pm$	$\pm$	$+$	$+$	$\pm$	$\pm$	$\pm$		6	3	
$+$	$\pm$	$\pm$	$\pm$	$+$	$-$	$\pm$	$\pm$	$\pm$		7	3	
$-$	$+$	$\pm$	$\pm$	$+$	$+$	$\pm$	$\pm$	$\pm$		7	3	
$-$	$+$	$\pm$	$\pm$	$+$	$-$	$\pm$	$\pm$	$\pm$		8	4	

gave the stability result ($u^{n,1} = -\tau p^n$)

$$\|u^n\|^2_{L^2(I)} + \|u^{n,1}\|^2_{L^2(I)} \leq \|u_0\|^2_{L^2(I)} + \|u^{0,1}\|^2_{L^2(I)},$$

which implies $\|u^n\|_{L^2(I)} \leq C\|u^0\|_{L^2(I)}$ with a constant $C > 1$. In this paper we claim the strong(3) stability and then get $\|u^n\|_{L^2(I)} \leq \|u^0\|_{L^2(I)}$ for $n \geq 3$.

So does for the LWDG(3,k) method [22] when the numerical flux parameters are taken from the second row in Table 3.2 with $\varepsilon = 1/2$.

4. Optimal error estimate. In this section we are devoted to obtain the optimal L^2-norm error estimate for the ESTDG method, which is stated in the following theorem.

THEOREM 4.1. *For the ESTDG(s, r, k) method* (2.6) *with the averaged numerical flux parameter $\Theta > 1/2$, we have the optimal error estimate*

$$\|u^N - U(t^N)\|_{L^2(I)} \leq C\|U_0\|_{H^{\natural+1}(I)}(h^{k+1} + \tau^r), \tag{4.1}$$

under the same type of temporal-spatial condition to ensure the L^2-norm stability, as stated in Theorems 3.1 through 3.3. Here $\natural = \max(k+1, r)$ and the bounding constant $C > 0$ is independent of h, τ and U_0.

For the special case that the numerical flux parameters are the same, this theorem has been proved in [25] for the fourth order in time RKDG method. Besides the above stability analysis, the major techniques to prove this theorem are the standard GGR projection with a fixed parameter and the good definition of the reference functions which are related to the local time marching of the exact solutions. However, this strategy does not work well for the ESTDG method with stage-dependent numerical flux parameters, because the GGR projection with the fixed parameter can not simultaneously eliminate the projection error at boundary endpoints and different time stage. We have to find a new approach to prove this theorem and obtain the optimal error estimate in both space and time.

4.1. Proof of Theorem 4.1. In this paper we propose a new analysis tool, named as *a series of space-time approximation functions* for any given spatial function, in order to set up a group of good reference functions and delicately define the stage errors for the fully discrete scheme. All approximation functions belong to the finite element space and are endowed with two properties. They perfectly match the local structure of the fully discrete method, and preserve the balance of the exact evolution under the control of the partial differential equation (PDE).

DEFINITION 4.1. *Let $W(x) \in L^2(I)$ be a given periodic function. Associated with the fully discrete ESTDG(s, r, k) method of the time step $\tau > 0$ and the finite element space V_h, there exists a series of space-time approximation functions, denoted by*

$$W_h^\ell = \mathbb{Q}_{h,\tau}^\ell W(x) \in V_h, \quad \ell = 0, 1, \ldots, s,$$

such that the following conditions hold:

- *Preserving the local structure of the fully discrete scheme, namely*

$$\Big(W_h^{\ell+1}, v\Big)_{I_h} = \sum_{0\leq\kappa\leq\ell}\Big[c_{\ell\kappa}\Big(W_h^\kappa, v\Big)_{I_h} + \tau d_{\ell\kappa}\mathcal{H}^{\theta_{\ell\kappa}}\big(W_h^\kappa, v\big)\Big], \quad \forall\, v \in V_h, \tag{4.2a}$$

  holds for $0 \leq \ell \leq s-1$;
- *Preserving the balance of the exact evolution under the control of* (1.1), *namely*

$$\Big(W_h^s - W_h^0, v\Big)_{I_h} = \Big(W(x-\tau\beta) - W(x), v\Big)_{I_h}, \quad \forall\, v \in V_h^\star. \tag{4.2b}$$

  Here $V_h^\star = \Big\{v \in V_h \colon (v,1)_{I_h} = 0\Big\}$ is the orthogonal complementary space of span$\{1\}$;
- *Conserving the overall mean for the head function W_h^0, namely*

$$\Big(W_h^0, 1\Big)_{I_h} = \Big(W(x), 1\Big)_{I_h}. \tag{4.2c}$$

Note that the last one W_h^s is named as the tail function.

In what follows we give some remarks to this definition. First of all, we point out that condition (4.2a) can be well understood by making full use of those concepts proposed in the matrix transferring process, for instance, the temporal differences of stage solutions and the associated evolution equation. That is to say, we have

$$W_h^s = \sum_{0\le\ell\le s} \alpha_\ell \mathbb{D}_\ell W_h \quad \text{with} \quad \mathbb{D}_\ell W_h = \sum_{0\le\kappa\le\ell} \sigma_{\ell\kappa} W_h^\kappa, \tag{4.3}$$

where $\alpha_\ell = \alpha_\ell(1)$ and $\sigma_{\ell\kappa} = \sigma_{\ell\kappa}(1)$ have been defined in (3.16) and (3.4), respectively. Analogously, we also have for $0 \le \ell \le s-1$ that

$$\Big(\mathbb{D}_{\ell+1} W_h, v\Big)_{I_h} = \tau \mathcal{H}^\vartheta(\mathbb{D}_\ell W_h, v) - \tau\beta \sum_{0\le\kappa\le\ell} q_{\ell,\kappa}(\vartheta) \Big\langle [\![\mathbb{D}_\kappa W_h]\!], [\![v]\!] \Big\rangle_{\Gamma_h}, \quad v \in V_h, \tag{4.4}$$

where $q_{\ell,\kappa}(\vartheta) = q_{\ell,\kappa}(1;\vartheta)$ has been defined in (3.11). Since $\mathcal{H}^\vartheta(\mathbb{D}_\ell W_h, 1) = 0$, by taking $v = 1$ in (4.4) we can inductively derive that

$$\Big(\mathbb{D}_\ell W_h, 1\Big)_{I_h} = 0, \quad \ell \ge 1. \tag{4.5}$$

Together with (4.3), this equality yields $(W_h^s - W_h^0, 1)_{I_h} = 0$. Due to the periodic boundary condition, we also have $(W(x-\tau\beta) - W(x), 1)_{I_h} = 0$. Consequently, condition (4.2b) can be extended to the whole finite element space, i.e.,

$$\Big(W_h^s - W_h^0, v\Big)_{I_h} = \Big(W(x-\tau\beta) - W(x), v\Big)_{I_h}, \quad \forall\, v \in V_h. \tag{4.6}$$

In the other words, condition (4.2c) ensures the uniqueness if the definition is made up of (4.2a) and (4.6).

It is worthy to emphasize that any space-time approximation function in Definition 4.1 is not a projection, even when the numerical flux parameters are the same. Below we give an example to show that. Let I_h be a given uniform mesh, and consider the function

$$W(x) = \sum_{1\le j\le J} L_{j,1}(x) \in V_h,$$

where $L_{j,1}(x) = (2x - x_{j-1/2} - x_{j+1/2})/h$ is the linear Legendre polynomial in I_j (with zero extension). Associated with the classical second order RKDG method [27] with $\theta_{\ell\kappa} \equiv 1$, we can yield the head function (with $\lambda = |\beta|\tau/h$)

$$W_h^0 = \frac{\lambda - 1}{3\lambda - 1} W \ne W.$$

This distinct property is bound to cause difficulties in obtaining the following lemma with respect to the approximation property.

Lemma 4.1. *For sufficiently small $\lambda = |\beta|\tau/h$, a series of the space-time approximation functions associated with the ESTDG(s,r,k) method are well defined, and further, if*

$$W(x) \in H^{\max(k+1,r+1)}(I),$$

the head function W_h^0 satisfies the optimal error estimate

$$\|W_h^0 - W\|_{L^2(I)} \le C\Big[h^{k+1}\|W\|_{H^\natural(I)} + \tau^r \|W\|_{H^r(I)}\Big]. \tag{4.7}$$

Here $\natural = \max(k+1, r)$ has been given in Theorem 4.1, and the bounding constant $C > 0$ is independent of h, τ and W.

For ease of reading, we postpone the lengthy and technical proof of this lemma to the next subsection and come back to prove Theorem 4.1 now. For any $n \le N$, we can utilize Definition 4.1 and define a series of space-time approximation functions

$$\chi^{n,\ell} = \mathbb{Q}^{\ell}_{h,\tau} U(x, t^n) \in V_h, \quad \ell = 0, 1, \dots, s. \tag{4.8}$$

We remark that $\chi^{n+1,0} \ne \chi^{n,s}$ in general, and the accumulation of these gaps at every time level forms the main error of the ESTDG method.

The reference functions are defined by those functions in (4.8) except $\ell = s$. For any n, denote the stage errors in the finite element space by

$$\xi^{n,\ell} = u^{n,\ell} - \chi^{n,\ell}, \quad \ell = 0, 1, \dots, s-1, \tag{4.9a}$$

and give a supplementary definition

$$\xi^{n,s} = \xi^{n+1,0} = \xi^{n+1}. \tag{4.9b}$$

Obviously, every $\chi^{n,\ell}$ in (4.8) satisfies the variation form (4.2a) with $W^{\ell}_h = \chi^{n,\ell}$. Subtracting them from the fully discrete method with the same n and ℓ, we obtain a series of error equations. Namely, for $\ell = 0, 1, \dots, s-1$, there holds

$$\Big(\xi^{n,\ell+1}, v\Big)_{I_h} = \sum_{0 \le \kappa \le \ell} \Big[c_{\ell\kappa} \Big(\xi^{n,\kappa}, v\Big)_{I_h} + \tau d_{\ell\kappa} \mathcal{H}^{\theta_{\ell\kappa}}(\xi^{n,\kappa}, v) \Big] + \tau \Big(F^{n,\ell}, v\Big)_{I_h}, \quad v \in V_h,$$

where the source term $F^{n,\ell}$ is equal to zero except the last one

$$F^{n,s-1} = \frac{1}{\tau}(\chi^{n,s} - \chi^{n+1,0}). \tag{4.10}$$

The above error equations have the same form as those in the nonhomogeneous ESTDG method. Along the similar line as in Section 3, we can get

$$\|\xi^N\|^2_{L^2(I)} \le C \Big[\|\xi^0\|^2_{L^2(I)} + \sum_{0 \le n < N} \|F^{n,s-1}\|^2_{L^2(I)} \tau \Big], \tag{4.11}$$

under the same type of temporal-spatial condition as stated in Theorems 3.1 through 3.3, where the bounding constant $C > 0$ is independent of h and τ, but may depend on the final time T.

It is easy to estimate each term on the right hand side of (4.11). It follows from the initial setting that $\xi^0 = \mathbb{P}_h U_0 - \mathbb{Q}^0_{h,\tau} U_0$. By using the triangle inequality, we have

$$\begin{aligned} \|\xi^0\|_{L^2(I)} &\le \|U_0 - \mathbb{P}_h U_0\|_{L^2(I)} + \|U_0 - \mathbb{Q}^0_{h,\tau} U_0\|_{L^2(I)} \\ &\le C \Big[h^{k+1} \|U_0\|_{H^{\natural}(I)} + \tau^r \|U_0\|_{H^r(I)} \Big], \end{aligned} \tag{4.12}$$

where the well-known approximation property of $\mathbb{P}_h$ and Lemma 4.1 are used separately. Since the time step is uniform, definition (4.2) implies that

$$\chi^{n+1,0} - \chi^{n,0} = \mathbb{Q}^0_{h,\tau}(U^{n+1} - U^n). \tag{4.13}$$

It follows from (4.6) that $(\chi^{n,s} - \chi^{n,0}, v)_{I_h} = (U^{n+1} - U^n, v)_{I_h}$. Hence (4.10) implies

$$\Big(F^{n,s-1}, v\Big)_{I_h} = \Big(\frac{U^{n+1} - U^n}{\tau}, v\Big)_{I_h} - \Big(\mathbb{Q}^0_{h,\tau}\Big(\frac{U^{n+1} - U^n}{\tau}\Big), v\Big)_{I_h},$$

which, together with Lemma 4.1 again, yields

$$\|F^{n,s-1}\|_{L^2(I)} \le C\left[h^{k+1}\left\|\frac{U^{n+1}-U^n}{\tau}\right\|_{H^\natural(I)} + \tau^r\left\|\frac{U^{n+1}-U^n}{\tau}\right\|_{H^r(I)}\right].$$

Since $U(x,t)=U_0(x-\beta t)$ and $U^{n+1}-U^n=\int_{t^n}^{t^{n+1}} U_t(x,t')\mathrm{d}t'$, we can obtain from the above inequality that

$$\|F^{n,s-1}\|_{L^2(I)} \le C\Big[h^{k+1}\|U_0\|_{H^{\natural+1}(I)} + \tau^r\|U_0\|_{H^{r+1}(I)}\Big]. \tag{4.14}$$

We can yield $\|\xi^N\|_{L^2(I)} \le C(h^{k+1}+\tau^r)\|U_0\|_{H^{\natural+1}(I)}$ by substituting (4.12) and (4.14) into (4.11). It follows from Lemma 4.1 that

$$\|U^N-\chi^{N,0}\|_{L^2(I)} \le C(h^{k+1}+\tau^r)\|U_0\|_{H^\natural(I)}.$$

Since $u^N-U^N=\xi^N-(U^N-\chi^{N,0})$, the above two inequalities and the triangle inequality complete the proof of Theorem 4.1.

Remark 4.1. *Due to (4.12), the initial solution can also be defined by the GGR projection and so on, provided that $\|U_0-u^0\|_{L^2(I)} \le C\|U_0\|_{H^\natural(I)}h^{k+1}$.*

4.2. Proof of Lemma 4.1. In Definition 4.1, the total number of the restrictions is equal to that of the unknowns' degrees of freedom. Hence it is sufficient and necessary to prove the uniqueness and existence by verifying that there is only one trivial solution $W_h^0=\cdots=W_h^s=0$ for $W=0$. The proofs of this topic and (4.7) are almost the same, so we solely present the latter in this subsection.

To do that, we need to introduce the GGR projection and the flux lifting function for any given parameter $\vartheta\neq 1/2$. For convenience, we first give the detailed definitions for $k\ge 1$ and then extend them to $k=0$ in Remark 4.2.

Definition 4.2. *Let $w(x)\in H^1(I)$ be a periodic function. The GGR projection, $\mathbb{G}_\vartheta w$, is defined as the unique function in V_h such that for $j=1,2,\ldots,J$,*

$$\int_{I_j}(\mathbb{G}_\vartheta w)v\mathrm{d}x = \int_{I_j} wv\mathrm{d}x \quad \forall\, v\in\mathcal{P}^{k-1}(I_j), \quad \text{and} \quad \{\!\{\mathbb{G}_\vartheta w\}\!\}_{j+\frac12}^{\vartheta} = \{\!\{w\}\!\}_{j+\frac12}^{\vartheta}. \tag{4.15}$$

Definition 4.3. *Let w^{b} be a single-valued periodic function defined on element endpoints. The flux lifting function, $\mathbb{L}_\vartheta w^{\mathrm{b}}$, is defined as the unique function in V_h such that for $j=1,2,\ldots,J$,*

$$\int_{I_j}(\mathbb{L}_\vartheta w^{\mathrm{b}})v\mathrm{d}x = 0 \quad \forall\, v\in\mathcal{P}^{k-1}(I_j), \quad \text{and} \quad \{\!\{\mathbb{L}_\vartheta w^{\mathrm{b}}\}\!\}_{j+\frac12}^{\vartheta} = w^{\mathrm{b}}_{j+\frac12}. \tag{4.16}$$

It has been proved in [3, Lemma 3.2] that the GGR projection is well-defined and satisfies

$$\|\mathbb{G}_\vartheta^\perp w\|_{L^2(I)} + h^{\frac12}\|(\mathbb{G}_\vartheta^\perp w)^\pm\|_{L^2(\varGamma_h)} \le Ch^{\min(\aleph,k+1)}\|w\|_{H^\aleph(I)}, \tag{4.17}$$

where $\mathbb{G}_\vartheta^\perp w = w-\mathbb{G}_\vartheta w$ is the projection error and $\aleph\ge 1$ is the smoothness requirement. The proof therein has implicitly used $\mathbb{G}_\vartheta w=\mathbb{P}_h w+\mathbb{L}_\vartheta\{\!\{w-\mathbb{P}_h w\}\!\}^\vartheta$ and shown that the flux lifting function is well-defined and satisfies

$$\|\mathbb{L}_\vartheta w^{\mathrm{b}}\|_{L^2(I)} \le Ch^{\frac12}\|w^{\mathrm{b}}\|_{L^2(\varGamma_h)}. \tag{4.18}$$

Furthermore, a direct application of Definitions 4.2 and 4.3 yields for any $v \in V_h$,

$$\mathcal{H}^\vartheta(\mathbb{G}_\vartheta^\perp w, v) = 0 \quad \text{and} \quad \mathcal{H}^\vartheta(\mathbb{L}_\vartheta w^{\mathrm{b}}, v) = \beta\Big\langle w^{\mathrm{b}}, [\![v]\!]\Big\rangle_{\Gamma_h}, \tag{4.19}$$

as well as the property on the overall mean

$$\Big(\mathbb{G}_\vartheta^\perp w, 1\Big)_{I_h} = 0 \quad \text{and} \quad \Big(\mathbb{L}_\vartheta w^{\mathrm{b}}, 1\Big)_{I_h} = 0. \tag{4.20}$$

Remark 4.2. *The above two definitions can be extended to $k = 0$ with some minor modifications such that the above four conclusions also hold. The process is divided into two steps:*

- *Define a unique function by the second condition in (4.15) and (4.16), respectively.*
- *Subtract a constant to get a modified function such that (4.20) holds.*

Now we begin to prove Lemma 4.1. Since $r \le s$ and $W(x) \in H^{r+1}(I)$, we would like to adopt the *cutting-off* technique [25, 24] and define a series of functions

$$\partial_\ell W = \begin{cases} (-\tau\beta\partial_x)^\ell\, W, & 0 \le \ell \le r-1, \\ 0, & r \le \ell \le s. \end{cases} \tag{4.21}$$

Every $\partial_\ell W \in H^2(I)$ at least, so the continuity is followed by the Sobolev embedding theorem. Using integration by parts, after some manipulations we can get the consistency property

$$\tau\mathcal{H}^\vartheta(\partial_\ell W, v) = \Big((-\tau\beta\partial_x)\partial_\ell W, v\Big)_{I_h}, \quad \forall v \in V_h. \tag{4.22}$$

Furthermore, the approximation property (4.17) with $\aleph = \max(k+1-\ell, 1)$ and the definition (4.21) show

$$\|\mathbb{G}_\vartheta^\perp(\partial_\ell W)\|_{L^2(I)} + h^{\frac12}\|(\mathbb{G}_\vartheta^\perp(\partial_\ell W))^\pm\|_{L^2(\Gamma_h)} \le Ch^{k+1}\|W\|_{H^\natural(I)}, \tag{4.23}$$

no matter whether $k+1 \ge r$ or not. Here and below we assume $\lambda \le 1$ without losing generality.

Let ϑ be the parameter used in the matrix transferring process, and assume $\vartheta \ne 1/2$. For $0 \le \ell \le s$, we define the error in the finite element space

$$\Xi_\ell^\vartheta = \mathbb{D}_\ell W_h - \mathbb{G}_\vartheta(\partial_\ell W) \in V_h, \tag{4.24}$$

which leads to the decomposition $\mathbb{D}_\ell W_h - \partial_\ell W = \Xi_\ell^\vartheta - \mathbb{G}_\vartheta^\perp(\partial_\ell W)$. Due to the triangle inequality and (4.23), it is sufficient to prove (4.7) by showing

$$\|\Xi_0^\vartheta\|_{L^2(I)} \le C\Big[h^{k+1}\|W\|_{H^\natural(I)} + \tau^r\|W\|_{H^r(I)}\Big], \tag{4.25}$$

with a special setting ϑ.

To complete this purpose, we have to set up two lemmas. The first one shows that the high order term can be mainly bounded by lower order term.

Lemma 4.2. *For any $\vartheta \ne \frac12$, there exists a bounding constant $C = C(\vartheta) > 0$ such that*

$$\|\Xi_{\ell+1}^\vartheta\|_{L^2(I)} \le C\lambda\|\Xi_0^\vartheta\|_{L^2(I)} + C\Big[h^{k+1}\|W\|_{H^\natural(I)} + \tau^r\|W\|_{H^r(I)}\Big] \tag{4.26}$$

holds for $0 \le \ell \le s-1$.

Proof. We can prove this lemma by (4.4), which is equivalent to condition (4.2a). By adding and subtracting some terms involving $\mathbb{G}_\vartheta(\partial_i W)$ three times, we have

$$\Big(\Xi^\vartheta_{\ell+1}, v\Big)_{I_h} = \mathcal{I}_1(v) + \mathcal{I}_2(v) + \mathcal{I}_3(v),$$

where

$$\begin{aligned}
\mathcal{I}_1(v) &= \tau\mathcal{H}^\vartheta\big(\Xi^\vartheta_\ell, v\big) - \tau\beta \sum_{0\le\kappa\le\ell} q_{\ell,\kappa}(\vartheta)\Big\langle [\![\Xi^\vartheta_\kappa]\!], [\![v]\!]\Big\rangle_{\Gamma_h},\\
\mathcal{I}_2(v) &= \tau\mathcal{H}^\vartheta(\mathbb{G}_\vartheta(\partial_\ell W), v) - \Big(\mathbb{G}_\vartheta(\partial_{\ell+1} W), v\Big)_{I_h},\\
\mathcal{I}_3(v) &= -\tau\beta \sum_{0\le\kappa\le\ell} q_{\ell,\kappa}(\vartheta)\Big\langle [\![\mathbb{G}_\vartheta(\partial_\kappa W)]\!], [\![v]\!]\Big\rangle_{\Gamma_h}.
\end{aligned}$$

In what follows we are going to estimate them one by one. Using (2.4c) for the first term, and using the Cauchy-Schwartz inequality and the inverse inequality (2.5) for the second term, we have

$$\mathcal{I}_1(v) \le C\lambda \sum_{0\le\kappa\le\ell} \|\Xi^\vartheta_\kappa\|_{L^2(I)}\|v\|_{L^2(I)}. \tag{4.27}$$

Due to (4.19) and (4.22), it follows from definition (4.21) that

$$\mathcal{I}_2(v) = \Big(-\tau\beta\partial_x(\partial_\ell W) - \mathbb{G}_\vartheta(\partial_{\ell+1}W), v\Big)_{I_h} = \begin{cases} \Big(\mathbb{G}^\perp_\vartheta(\partial_{\ell+1}W), v\Big)_{I_h}, & 0\le\ell\le r-2,\\ \Big(-\tau\beta\partial_x(\partial_\ell W), v\Big)_{I_h}, & \ell = r-1,\\ 0, & \text{otherwise.}\end{cases}$$

Using (4.23) for the first case and (4.21) for the second case, respectively, an application of Cauchy-Schwartz inequality yields a unified inequality

$$\mathcal{I}_2(v) \le C\Big[h^{k+1}\|W\|_{H^\natural(I)} + \tau^r\|W\|_{H^r(I)}\Big]\|v\|_{L^2(I)}. \tag{4.28}$$

Since $[\![\partial_\kappa W]\!] = 0$ and $\lambda \le 1$, we can use (4.23) and (2.5) to get

$$\mathcal{I}_3(v) = \tau\beta \sum_{0\le\kappa\le\ell} q_{\ell,\kappa}(\vartheta)\Big\langle [\![\mathbb{G}^\perp_\vartheta(\partial_\kappa W)]\!], [\![v]\!]\Big\rangle_{\Gamma_h} \le Ch^{k+1}\|W\|_{H^\natural(I)}\|v\|_{L^2(I)}. \tag{4.29}$$

Summing up the above three conclusions and taking $v = \Xi^\vartheta_{\ell+1} \in V_h$, we finally obtain

$$\|\Xi^\vartheta_{\ell+1}\|_{L^2(I)} \le C\lambda \sum_{0\le\kappa\le\ell}\|\Xi^\vartheta_\kappa\|_{L^2(I)} + C\Big[h^{k+1}\|W\|_{H^\natural(I)} + \tau^r\|W\|_{H^r(I)}\Big],$$

for $0 \le \ell \le s-1$. This completes the proof of this lemma. ∎

Below we set up another lemma by condition (4.6). Substitute (4.3) into the left hand side (LHS) of this condition and expand each term by the relationship (4.4). By changing the summation orders for those terms on element boundaries, we can easily get

$$\begin{aligned}
\text{LHS} &= \tau \sum_{0\le\ell\le s-1} \alpha_{\ell+1}\mathcal{H}^\vartheta(\mathbb{D}_\ell W_h, v) - \tau\beta\sum_{0\le\kappa\le s-1}\psi_\kappa(\vartheta)\Big\langle [\![\mathbb{D}_\kappa W_h]\!], [\![v]\!]\Big\rangle_{\Gamma_h}\\
&= \tau\mathcal{H}^\vartheta\left(\sum_{0\le\ell\le s-1}\Big[\alpha_{\ell+1}\mathbb{D}_\ell W_h - \psi_\ell(\vartheta)\mathbb{L}_\vartheta[\![\mathbb{D}_\ell W_h]\!]\Big], v\right),
\end{aligned} \tag{4.30}$$

where the second identity in (4.19) is used at the last step, and

$$\psi_\kappa(\vartheta) = \sum_{\kappa\le\ell\le s-1} \alpha_{\ell+1} q_{\ell,\kappa}(\vartheta). \tag{4.31}$$

We remark that $\psi_0(\vartheta)$ plays an important role in the remaining analysis, especially when ϑ is taken as the averaged numerical flux parameter Θ. The essential property is stated in the following proposition.

PROPOSITION 4.1. *There holds $\psi_0(\Theta) = 0$.*

Proof. Due to Lemma 3.3 we have $\Theta = \Theta(1)$. Since $\alpha_1(1) = 1$, we can get from (3.14), (3.28) and (4.31) that $\psi_0(\vartheta) = \Theta - \vartheta$. Hence this proposition is proved. ◻

Now we are going to deal with the right hand side (RHS) of condition (4.6). An application of the Taylor expansion up to rth order derivative yields

$$W(x-\tau\beta) - W(x) = (-\tau\beta\partial_x)\left[\sum_{0\le\ell\le r-1} \frac{1}{(\ell+1)!}\partial_\ell W(x) + \widetilde{W}(x)\right], \tag{4.32}$$

with the truncation function

$$\widetilde{W}(x) = \frac{1}{r!(\tau\beta)}\int_0^{\tau\beta} \partial_x^r W(x-\tilde{x})(\tilde{x}-\tau\beta)^r \mathrm{d}\tilde{x}.$$

It is easy to see that $(\widetilde{W}, 1)_{I_h} = 0$ and

$$\|\widetilde{W}\|_{L^2(I)} \le C\tau^r \|W\|_{H^r(I)}. \tag{4.33}$$

By integration by part for the definition of $\widetilde{W}(x)$, we are able to drop the derivative order of $W(\cdot)$ and get

$$\|\widetilde{W}\|_{H^\sharp(I)} \le C\tau^{r-1}\|W\|_{H^\natural(I)}, \quad \text{with } \sharp = \max(k+2-r, 1). \tag{4.34}$$

As we have mentioned in (3.17), we know $\alpha_{\ell+1}(m) = 1/(\ell+1)!$ for $\ell \le r-1$. Substituting (4.32) into RHS and using the consistency property (4.22) for both $\partial_\ell W$ and $\widetilde{W}$, we can obtain from (4.19) that

$$\mathrm{RHS} = \tau\mathcal{H}^\vartheta\left(\sum_{0\le\ell\le s-1} \alpha_{\ell+1}\mathbb{G}_\vartheta(\partial_\ell W) + \mathbb{G}_\vartheta\widetilde{W}, v\right). \tag{4.35}$$

Here the range of summation index is expanded, since $\partial_\ell W = 0$ for $\ell \ge r$, due to (4.21).

Due to (4.30) and (4.35), it follows from condition (4.6) that

$$\varrho^\vartheta \overset{\text{def}}{=} \sum_{0\le\ell\le s-1}\left[\alpha_{\ell+1}\Xi_\ell^\vartheta - \psi_\ell(\vartheta)\mathbb{L}_\vartheta[\![\mathbb{D}_\ell W_h]\!]\right] - \mathbb{G}_\vartheta\widetilde{W} \in V_h \tag{4.36}$$

satisfies the variational form $\mathcal{H}^\vartheta(\varrho^\vartheta, v) = 0$ for any $v \in V_h$. By successively taking $v = \varrho^\vartheta$ and $v = \partial_x\varrho^\vartheta$, we can see that ϱ^ϑ must be a constant. This concludes

$$\varrho^\vartheta = 0, \tag{4.37}$$

if the overall mean is equal to zero. By (4.20), we have $(\mathbb{L}_\vartheta[\![\mathbb{D}_\ell W_h]\!], 1)_{I_h} = 0$ for $\ell \geq 0$, and

$$(\mathbb{G}_\vartheta \widetilde{W}, 1)_{I_h} = (\widetilde{W}, 1)_{I_h} = 0.$$

Furthermore, we also have $(\Xi_\ell^\vartheta, 1)_{I_h} = 0$ due to the following facts:

- For $\ell = 0$, condition (4.2c) implies $(W_h^0, 1)_{I_h} = (W, 1)_{I_h} = (\mathbb{G}_\vartheta W, 1)_{I_h}$;
- For $\ell \geq 1$, the periodicity means $(\mathbb{G}_\vartheta(\partial_\ell W), 1)_{I_h} = (\partial_\ell W, 1)_{I_h} = 0$, and (4.5) shows $(\mathbb{D}_\ell W_h, 1)_{I_h} = 0$.

Summing up the above verifications, we conclude that (4.37) is true.

LEMMA 4.3. *Let $\vartheta = \Theta$, then we have*

$$\|\Xi_0^\vartheta\|_{L^2(I)} \leq C \sum_{1\leq \ell \leq s-1} \|\Xi_\ell^\vartheta\|_{L^2(I)} + C\Big[h^{k+1}\|W\|_{H^\natural(I)} + \tau^r \|W\|_{H^r(I)}\Big]. \tag{4.38}$$

Proof. Thanks to Proposition 4.1, we can get rid of the trouble term $\mathbb{L}_\vartheta[\![\mathbb{D}_0 W_h]\!]$ in (4.36). Then it follows from (4.37) and $\alpha_1 = 1$ that

$$\|\Xi_0^\vartheta\|_{L^2(I)} \leq C \sum_{1\leq \ell\leq s-1} \|\Xi_\ell^\vartheta\|_{L^2(I)} + C \sum_{1\leq \ell\leq s-1} \|\mathbb{L}_\vartheta[\![\mathbb{D}_\ell W_h]\!]\|_{L^2(I)} + C\|\mathbb{G}_\vartheta \widetilde{W}\|_{L^2(I)}. \tag{4.39}$$

It is easy to estimate the last two terms. Since $[\![\mathbb{D}_\ell W_h]\!] = [\![\mathbb{D}_\ell W_h - \partial_\ell W]\!] = [\![\Xi_\ell^\vartheta]\!] - [\![\mathbb{G}_\vartheta^\perp \partial_\ell W]\!]$, it follows from (4.18) and the triangle inequality that

$$\|\mathbb{L}_\vartheta[\![\mathbb{D}_\ell W_h]\!]\|_{L^2(I)} \leq Ch^{\frac{1}{2}}\|[\![\Xi_\ell^\vartheta]\!]\|_{L^2(\Gamma_h)} + Ch^{\frac{1}{2}}\|[\![\mathbb{G}_\vartheta^\perp \partial_\ell W]\!]\|_{L^2(\Gamma_h)}.$$

Together with (2.5) and (4.23) for each term, this deduces

$$\|\mathbb{L}_\vartheta[\![\mathbb{D}_\ell W_h]\!]\|_{L^2(I)} \leq C\|\Xi_\ell^\vartheta\|_{L^2(I)} + Ch^{k+1}\|W\|_{H^\natural(I)}. \tag{4.40}$$

By the triangle inequality and (4.17), we have

$$\|\mathbb{G}_\vartheta \widetilde{W}\|_{L^2(I)} \leq \|\widetilde{W}\|_{L^2(I)} + \|\mathbb{G}_\vartheta^\perp \widetilde{W}\|_{L^2(I)} \leq \|\widetilde{W}\|_{L^2(I)} + Ch^\sharp\|\widetilde{W}\|_{H^\sharp(I)}.$$

The two terms on the right hand side are bounded by (4.33) and (4.34), respectively. Since $\lambda \leq 1$, we can get the unified inequality

$$\|\mathbb{G}_\vartheta \widetilde{W}\|_{L^2(I)} \leq C\Big[h^{k+1}\|W\|_{H^\natural(I)} + \tau^r\|W\|_{H^r(I)}\Big]. \tag{4.41}$$

Substituting (4.40) and (4.41) into (4.39) completes the proof of this lemma. ∎

Till now (4.25) is implied by collecting Lemmas 4.2 and 4.3 if λ is small enough. This completes the proof of Lemma 4.1 and ends this subsection.

5. Numerical experiments.

In this section we present some numerical experiments to verify the proposed theoretical results. Let $\beta = 1$ and $T = 1$ in (1.1) for all tests. All schemes are taken from the two examples given in Section 3.

5.1. Verification on stability results.

Take the uniform meshes with $J = 64$, as an example. With standard orthogonal basis of the finite element space, the ESTDG method is written into $\widetilde{\boldsymbol{u}}^{n+1} = \mathbb{K}\widetilde{\boldsymbol{u}}^n$, where $\widetilde{\boldsymbol{u}}^n$ is the vector made up of the expansion coefficients of u^n. The spectral norm $\|\mathbb{K}^m\|_2$ describes the L^2-norm amplification every m step time marching [27].

5.1.1. The RKDG method. Consider the RKDG$(4,4,k)$ method and the numerical flux parameters are given by (3.34), where $\varepsilon = 0.25, 0.50, 0.75$ and $y = 1, 3$. In Figures 5.1 and 5.2 we plot

$$\max(\|\mathbb{K}^m\|_2^2 - 1, 10^{-16})$$

for different λ in the logarithmic coordinates, with $k = 1, 2, 3$ from left to right.

- For $y = 3$, this quantity is always close to 10^{-16} and thus implies the monotonicity stability.
- For $y = 1$, the data points increase along the line of slope 5 only for $k \geq 2$ and $m = 1$. These numerical results show the strong(2) stability at least and the monotonicity stability for $k \leq 1$.

This verifies what we have stated in subsection 3.2.1.

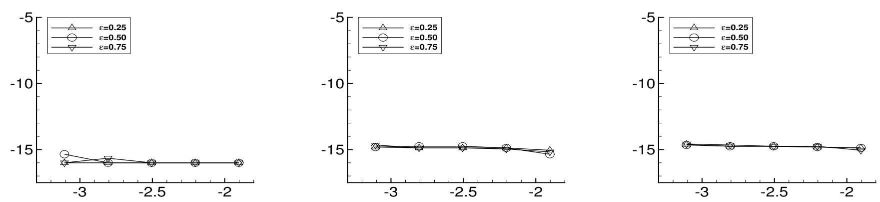

(a) $m = 1$

FIG. 5.1. *The L^2-norm amplification of the RKDG$(4,4,k)$ solutions every m-step: $k = 1, 2, 3$ from left to right. Here $\varepsilon = 0.25, 0.50, 0.75$ and $y = 3$.*

To show the difference between the strong stability and the monotonicity stability, we take $k = 3$ as an example and plot in Figure 5.3 the L^2-norm evolution at the first twelve steps, where $\lambda = 0.02$ and $\varepsilon = 0.50$. The initial solution is taken as the first unit singular vector of $\mathbb{K}$. For $y = 1$, we can see in the left picture that the L^2-norm overshoots at the first step and decreases every two and three steps. But for $y = 3$, the monotonicity stability is clearly observed in the right picture. This verifies our theoretical results given in subsection 3.2.1.

5.1.2. The LWDG method. Consider the LWDG$(2,k)$ method. As an example, we take the numerical flux parameters as $\theta_{00} = \theta_{10} = 1/2 + \varepsilon$ and $\theta_{11} = 1/2 - \varepsilon$, where $\varepsilon = 0.25, 0.50, 0.75$. We plot in Figure 5.4 some pictures for $k = 0, 1, 2$ and $m = 1, 2, 3, 4, 5$.

- If $k = 0$, this quantity is close to 10^{-16} and shows the monotonicity stability.
- If $k = 1$, the data points increase along the line of slope 3 for $m \leq 2$ but this quantity is close to 10^{-16} for $m \geq 3$. This verifies the strong(3) stability for $k = 1$.
- If $k = 2$, the data points increase with slope 3 (odd) for $m \leq 2$ and with slope 4 (even) for $m \geq 3$. This shows the weak(4) stability.

The above observations well support the results listed in Table 3.1.

In Figure 5.5, the left picture plots the L^2-norm evolution of the LWDG$(2,1)$ solution at the previous twelve steps, where $\lambda = 0.02$ and $\varepsilon = 0.50$. The initial solution is taken as the first unit singular vector of $\mathbb{K}^2$. We can see that the monotonicity decreasing is lost at the first two steps and conclude that the scheme can not have the strong(2) stability. As a comparison, we also plot in the right picture for the LWDG(2,1) method with $\theta_{11} = 1/2 + \varepsilon$ and the others are kept the same. We can see the monotonicity stability for this case.

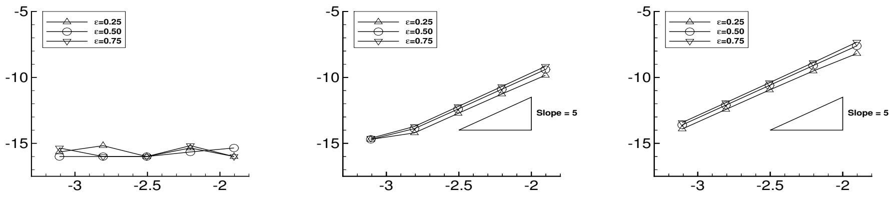

(a) $m = 1$

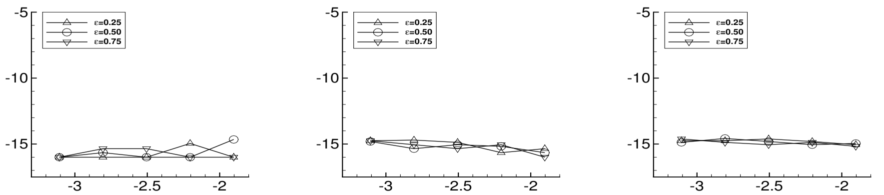

(b) $m = 2$

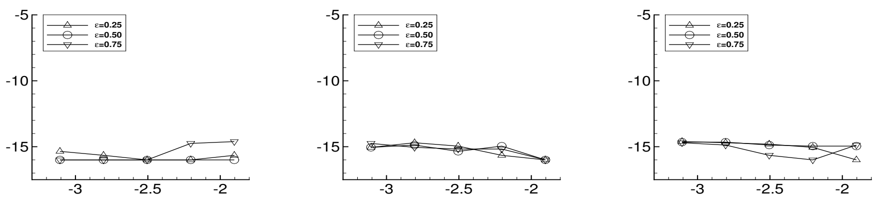

(c) $m = 3$

FIG. 5.2. *The L^2-norm amplification of the RKDG$(4, 4, k)$ solutions every m-step: $k = 1, 2, 3$ from left to right. Here $\varepsilon = 0.25, 0.50, 0.75$ and $y = 1$.*

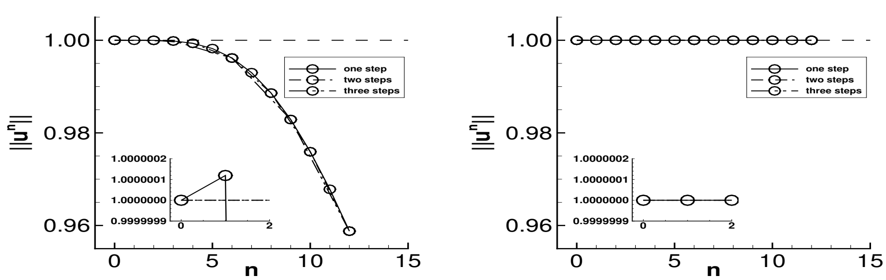

FIG. 5.3. *The L^2-norm evolution for the RKDG$(4, 4, 3)$ method. Left: $y = 1$. Right: $y = 3$. Here $\lambda = 0.02$ and $\varepsilon = 0.50$.*

5.2. Verification on the error estimate. In this subsection we investigate the numerical accuracy of the ESTDG method with two initial solutions. Since the numerical results are almost the same, we only present the experiment data for the RKDG(4,4,k) method on nonuniform mesh, which is constructed by perturbing the uniform mesh nodes randomly by at most 10%. Take the time step by $\tau = 0.05h_{\min}$

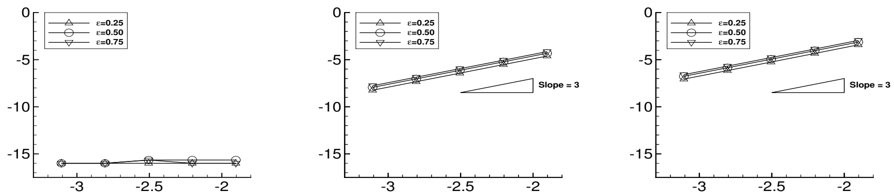

(a) $m = 1$

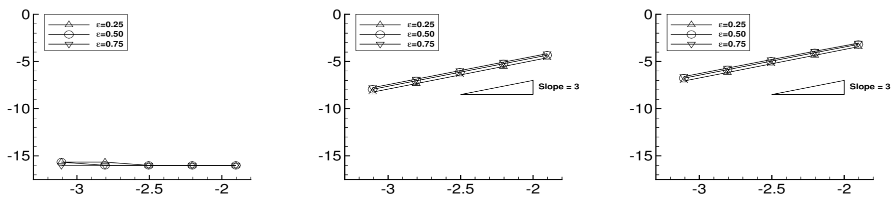

(b) $m = 2$

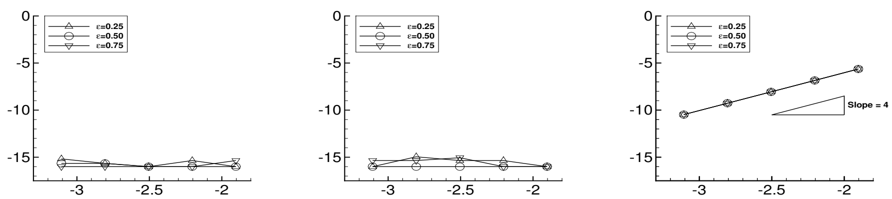

(c) $m = 3$

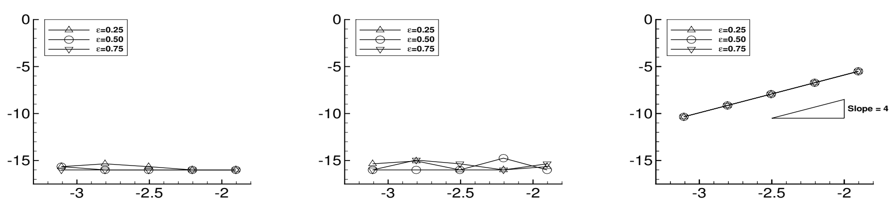

(d) $m = 4$

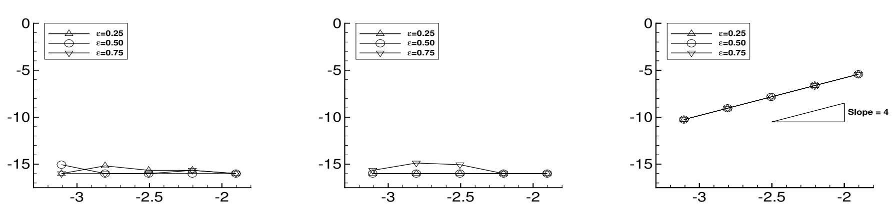

(e) $m = 5$

FIG. 5.4. *The L^2-norm amplification of the LWDG$(2,k)$ solution every m-step: $\theta_{00} = \theta_{10} = 1/2 + \varepsilon$ and $\theta_{11} = 1/2 - \varepsilon$. Here $k = 0, 1, 2$ from left to right and $\varepsilon = 0.25, 0.50, 0.75$.*

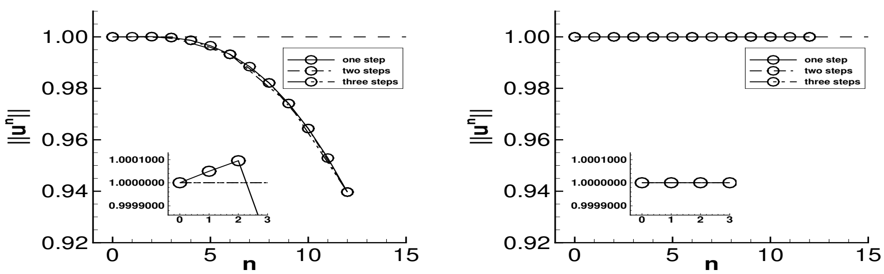

FIG. 5.5. *The L^2-norm evolution for the LWDG$(2,1)$ method. Left: $\theta_{11}=0$; Right: $\theta_{11}=1$. Here $\lambda=0.02$ and $\theta_{00}=\theta_{10}=1$.*

in what follows, where $h_{\min}$ is the minimal length.

First we consider a sufficiently smooth initial solution, for example,

$$U_0(x)=\sin(2\pi x).$$

In Tables 5.1 and 5.2, we give the error and convergence order in the L^2-norm for $y=3$ and $y=1$ respectively. We can clearly observe the optimal convergence order, which supports the result in Theorem 4.1.

TABLE 5.1
The L^2-norm errors and convergence orders of the RKDG$(4,4,k)$ method with the numerical flux parameter (3.34) and $y=3$. Nonuniform mesh.

	J	$\varepsilon=0.25$		$\varepsilon=0.50$		$\varepsilon=0.75$	
		Error	Order	Error	Order	Error	Order
	160	7.32E-05		5.28E-05		4.90E-05	
	320	1.83E-05	2.00	1.31E-05	2.01	1.24E-05	1.98
$k=1$	640	4.56E-06	2.00	3.32E-06	1.99	3.09E-06	2.00
	1280	1.14E-06	2.00	8.27E-07	2.00	7.73E-07	2.00
	2560	2.85E-07	2.00	2.07E-07	2.00	1.93E-07	2.00
	160	2.11E-07		3.42E-07		4.91E-07	
	320	2.67E-08	2.98	4.27E-08	3.00	6.17E-08	2.99
$k=2$	640	3.34E-09	3.00	5.32E-09	3.01	7.68E-09	3.01
	1280	4.18E-10	3.00	6.66E-10	3.00	9.60E-10	3.00
	2560	5.23E-11	3.00	8.32E-11	3.00	1.20E-10	3.00
	160	6.03E-10		4.88E-10		5.21E-10	
	320	3.71E-11	4.02	2.99E-11	4.03	2.96E-11	4.14
$k=3$	640	2.31E-12	4.01	1.90E-12	3.98	1.83E-12	4.01
	1280	1.44E-13	4.00	1.16E-13	4.03	1.16E-13	3.98
	2560	8.95E-15	4.01	7.26E-15	4.00	7.34E-15	3.98

Next we investigate the smoothness requirement proposed in this paper. To do that, we take the initial solution

$$U_0(x)=[\sin(2\pi x)]^{\epsilon+2/3},$$

and ϵ is a positive integer. This function belongs to $H^{\epsilon+1}(I)$, but not $H^{\epsilon+2}(I)$. In Table 5.3, the optimal convergence order is observed when $\epsilon=r$, but not $\epsilon=r-1$. This indicates that the smoothness requirement in Theorem 4.1 appears to be sharp.

6. Conclusion. In this paper we have presented the L^2-norm stability analysis and the optimal error estimate for the ESTDG method, which adopts the explicit

TABLE 5.2

The L^2-norm errors and convergence orders of the RKDG$(4,4,k)$ method with the numerical flux parameter (3.34) *and $y=1$. Nonuniform mesh.*

	J	$\varepsilon=0.25$		$\varepsilon=0.50$		$\varepsilon=0.75$	
		Error	Order	Error	Order	Error	Order
$k=1$	160	8.03E-05		5.55E-05		4.99E-05	
	320	2.01E-05	2.00	1.39E-05	2.00	1.24E-05	2.01
	640	5.01E-06	2.00	3.47E-06	2.00	3.13E-06	1.98
	1280	1.25E-06	2.00	8.67E-07	2.00	7.87E-07	1.99
	2560	3.13E-07	2.00	2.17E-07	2.00	1.97E-07	2.00
$k=2$	160	2.03E-07		4.83E-10		4.22E-07	
	320	2.49E-08	3.03	3.03E-11	3.99	5.31E-08	2.99
	640	3.13E-09	2.99	1.91E-12	3.99	6.64E-09	3.00
	1280	3.91E-10	3.00	1.18E-13	4.01	8.30E-10	3.00
	2560	4.94E-11	2.99	7.44E-15	3.99	1.04E-10	3.00
$k=3$	160	6.48E-10		4.83E-10		4.78E-10	
	320	3.92E-11	4.05	3.03E-11	3.99	2.91E-11	4.04
	640	2.49E-12	3.98	1.91E-12	3.99	1.86E-12	3.97
	1280	1.58E-13	3.98	1.18E-13	4.01	1.15E-13	4.02
	2560	9.78E-15	4.01	7.44E-15	3.99	7.23E-15	3.99

TABLE 5.3

The L^2-norm errors and convergence orders of the RKDG$(4,4,3)$ method on nonuniform mesh. Here $\epsilon = r-1$ on the left column and $\epsilon = r$ on the right column.

		RKDG(4,4,3), $y=3$				RKDG(4,4,3), $y=1$			
$\varepsilon=0.25$	160	3.87E-08		2.20E-08		3.70E-08		2.43E-08	
	320	3.06E-09	3.66	1.37E-09	4.00	2.92E-09	3.66	1.52E-09	4.00
	640	2.45E-10	3.64	8.57E-11	4.00	2.35E-10	3.64	9.51E-11	4.00
	1280	1.97E-11	3.64	5.35E-12	4.00	1.91E-11	3.62	5.94E-12	4.00
	2560	1.59E-12	3.63	3.34E-13	4.00	1.55E-12	3.62	3.71E-13	4.00
$\varepsilon=0.50$	160	5.24E-08		1.66E-08		4.82E-08		1.74E-08	
	320	4.05E-09	3.69	1.02E-09	4.02	3.76E-09	3.68	1.08E-09	4.01
	640	3.12E-10	3.70	6.36E-11	4.01	2.93E-10	3.68	6.72E-11	4.01
	1280	2.41E-11	3.70	3.97E-12	4.00	2.28E-11	3.68	4.19E-12	4.00
	2560	1.85E-12	3.70	2.48E-13	4.00	1.77E-12	3.68	2.62E-13	4.00
$\varepsilon=0.75$	160	6.45E-08		1.56E-08		5.82E-08		1.59E-08	
	320	4.82E-09	3.74	9.55E-10	4.03	4.43E-09	3.72	9.78E-10	4.03
	640	3.62E-10	3.74	5.91E-11	4.01	3.37E-10	3.72	6.07E-11	4.01
	1280	2.73E-11	3.73	3.68E-12	4.01	2.56E-11	3.71	3.78E-12	4.00
	2560	2.07E-12	3.72	2.30E-13	4.00	1.96E-12	3.71	2.36E-13	4.00

single-step time-marching and the stage-dependent numerical flux parameters in the DG discretization. The main tool is the technique of the matrix transferring process based on the temporal difference of the stage solutions, where the averaged numerical flux parameter is proposed to measure the upwind effect in the fully discrete schemes. By a unified analysis framework, in this paper we give some detailed L^2-norm stability stability results for the RKDG method with downwind treatments and the LWDG method with different numerical flux parameters for the auxiliary variables. In order to obtain the optimal error estimate for the ESTDG method, we propose a series of space-time approximation functions for any given spatial function and then establish a new proof line for the fully discrete method. During this procedure, the technique of the matrix transferring process and the averaged numerical flux parameter play very important roles. In future work, we will extend the above works to variable-coefficient linear hyperbolic problems and nonlinear conservation laws in one and/or multidimensional cases.

7. Appendix.

In this section we give some supplemental materials for those conclusions unproved in Section 3. To this end, we have to make a matrix description of the matrix transferring process.

Associated with the multistep number m and the stage number s, we introduce some column vectors and square matrices of size ms, whose component is only either 0 or 1. More specifically, let $\mathbf{1}(m,s) = (1,1,\dots,1)^\top$ and $\boldsymbol{e}_i(m,s)$, for $i = 0,1,2,\dots,ms-1$, be the unit vector which has 1 only at the i-th position. Let $\underline{\boldsymbol{I}}(m,s)$ be the identity matrix and $\underline{\boldsymbol{E}}(m,s)$ the shifting matrix which has 1 only at the lower second diagonal line. Let

$$\underline{\boldsymbol{L}}(m,s) = \Big[\underline{\boldsymbol{I}}(m,s) - \underline{\boldsymbol{E}}(m,s)\Big]^{-1} - \underline{\boldsymbol{I}}(m,s) = \sum_{1\le\kappa\le ms-1} \underline{\boldsymbol{E}}(m,s)^\kappa,$$

which has 1 at the strictly lower region. For simplicity of notations, we would like to denote, for example

$$\mathbf{1}(m) = \mathbf{1}(m,s), \quad \mathbf{1} = \mathbf{1}(1,s), \quad \hat{\mathbf{1}} = \mathbf{1}(m,1).$$

This rule will be used throughout the entire section.

7.1. Matrix description of matrix transferring process.

In this subsection we present a matrix description of how to get the ultimate spatial matrix. To do that, we define some ms order matrices

$$\underline{\boldsymbol{C}}(m) = \{c_{ij}(m)\}, \quad \underline{\boldsymbol{D}}(m) = \{d_{ij}(m)\}, \quad \underline{\boldsymbol{W}}(m;\vartheta) = \{d_{ij}(m)(\theta_{ij}(m) - \vartheta)\}, \tag{7.1a}$$

and

$$\underline{\boldsymbol{\Sigma}}(m) = \{\sigma_{ij}(m)\}, \quad \underline{\boldsymbol{\Phi}}(m) = \{\phi_{ij}(m)\}, \quad \underline{\boldsymbol{Q}}(m;\vartheta) = \{q_{ij}(m;\vartheta)\}. \tag{7.1b}$$

Here i and j are all taken from 0 to $ms-1$, and ϑ is the given parameter as mentioned in subsection 3.1.1.

7.1.1. The ultimate spatial matrix.

This matrix is obtained by running Algorithm 1 for $\ell = 1,2,\dots,\zeta$, where the crucial calculation is the increment accumulation in Step 2.

Define a lower triangle matrix $\underline{\boldsymbol{A}}^\star(m) = \{a^\star_{ij}(m)\}_{0\le i,j\le ms-1}$, whose entries are defined as zero except

$$a^\star_{ij}(m) = (1-\delta_{ij}/2)a^{(j)}_{i+1,j}(m), \quad \text{for } j \le i \le ms-1, \quad \text{and } 0 \le j \le \zeta - 1.$$

Noticing that $\{\tilde{q}_{ij}(m)\}_{0\le i,j,\le ms-1}$ is a lower triangle matrix, we can extend all three summation ranges in Step 2 to the entire index set $\{0,1,\dots,ms-1\}$. Gathering up the related operation of Algorithm 1 till the matrix transferring process stops, we can easily obtain a unified description for the increment procedure at any fixed position. More specifically, the integrated calculation reads (dropping (m) for convenience)

$$g_{i'j'} \leftarrow g_{i'j'} - a^\star_{i'j'}; \quad g_{i'j'} \leftarrow g_{i'j'} + a^\star_{\kappa'j'}\tilde{q}_{\kappa'i'}, \quad g_{i'j'} \leftarrow g_{i'j'} + a^\star_{i'\kappa'}\tilde{q}_{\kappa'j'},$$

where the index i', j' and κ' go through $\{0,1,\dots,ms-1\}$. Finally, the total increment at Step 2 of Algorithm 1 can be expressed in the matrix form

$$\underline{\boldsymbol{G}}(m) = (2\vartheta-1)\underline{\boldsymbol{A}}^\star(m) + \underline{\boldsymbol{Q}}(m;\vartheta)^\top\underline{\boldsymbol{A}}^\star(m) + \underline{\boldsymbol{A}}^\star(m)\underline{\boldsymbol{Q}}(m;\vartheta),$$

where $\tilde{q}_{ij}(m) = q_{ij}(m;\vartheta) + \vartheta\delta_{ij}$ is used.

From Step 3 of Algorithm 1, we have the ultimate spatial matrix (the last row and column is dropped, since they are always zero)

$$\begin{aligned}\mathbb{B}(m) &= \underline{\boldsymbol{G}}(m) + \underline{\boldsymbol{G}}(m)^\top \\ &= \Big(\vartheta - \frac{1}{2}\Big)\underline{\boldsymbol{B}}^\star(m) + \frac{1}{2}\Big[\underline{\boldsymbol{B}}^\star(m)\underline{\boldsymbol{Q}}(m;\vartheta) + \underline{\boldsymbol{Q}}(m;\vartheta)^\top\underline{\boldsymbol{B}}^\star(m)\Big].\end{aligned} \tag{7.2}$$

Here we have introduced a symmetric matrix

$$\underline{\boldsymbol{B}}^\star(m) = 2\underline{\boldsymbol{A}}^\star(m) + 2\underline{\boldsymbol{A}}^\star(m)^\top = \{b^\star_{ij}(m)\}_{0\le i,j\le ms-1}, \tag{7.3}$$

which is the same as that in [24]. The entry at the lower triangular zone is defined as

$$b^\star_{ij}(m) = \begin{cases} 2a^{(j)}_{i+1,j}(m), & 0 \le j \le \zeta-1,\ j \le i \le ms-1, \\ 0, & \text{otherwise.}\end{cases} \tag{7.4}$$

In what follows, we only need to pay more attention on the perturbation matrix

$$\underline{\boldsymbol{Z}}(m;\vartheta) = \underline{\boldsymbol{B}}^\star(m)\underline{\boldsymbol{Q}}(m;\vartheta) = \{z_{ij}(m;\vartheta)\}_{0\le i,j\le ms-1}. \tag{7.5}$$

7.1.2. Elemental formula on the perturbation matrix. Taking into account the purpose of the matrix transferring process, we want to deduce a convenient and unified formula for those left-top entries $z_{ij}(m;\vartheta)$ for $0 \le i,j \le \zeta-1$. To do that, we have to rebuild an equivalent formula for some $b^\star_{ij}(m)$.

Lemma 7.1. *Denote $\alpha_i(m) = 0$ if $i > ms$ for simplicity. For $0 \le i \le \zeta-1$, there holds*

$$b^\star_{ij}(m) = 2\sum_{0\le\kappa\le i}(-1)^\kappa\alpha_{i-\kappa}(m)\alpha_{j+1+\kappa}(m), \quad 0 \le j \le ms-1. \tag{7.6}$$

Proof. Recalling the existing results [24, Lemma 3.1]:

$$a^{(j')}_{i'j'}(m) = \sum_{0\le\kappa\le j'}(-1)^\kappa\alpha_{i'+\kappa}(m)\alpha_{j'-\kappa}(m), \quad \text{for } 0 \le j' \le \zeta \text{ and } j' < i' \le ms, \tag{7.7a}$$

$$a^{(i')}_{i'i'}(m) = \sum_{-i'\le\kappa\le i'}(-1)^\kappa\alpha_{i'+\kappa}(m)\alpha_{i'-\kappa}(m), \quad \text{for } 1 \le i' \le \zeta, \tag{7.7b}$$

we can prove this lemma by some simple discussions for different case of j.

If $j > i$, since $\mathbb{B}^\star(m)$ is symmetric, it follows from (7.4) that

$$b^\star_{ij}(m) = b^\star_{ji}(m) = 2a^{(i)}_{j+1,i}(m).$$

This proves (7.6) by using the first equation in (7.7) with $i' = j+1$ and $j' = i$.

Otherwise, if $j \le i$, we similarly have

$$b^\star_{ij}(m) = 2a^{(j)}_{i+1,j}(m) = 2\sum_{0\le\kappa\le j}(-1)^\kappa\alpha_{i+1+\kappa}(m)\alpha_{j-\kappa}(m).$$

To prove this lemma, we just need to show $\Upsilon = 0$, with

$$\Upsilon \overset{\text{def}}{=} \sum_{0\le\kappa\le j} (-1)^\kappa \alpha_{i+1+\kappa}(m)\alpha_{j-\kappa}(m) - \sum_{0\le\kappa\le i} (-1)^\kappa \alpha_{i-\kappa}(m)\alpha_{j+1+\kappa}(m)$$
$$= \sum_{0\le\kappa\le j+i+1} (-1)^{j-\kappa}\alpha_\kappa(m)\alpha_{j+i+1-\kappa}(m).$$

Here we have respectively used the replacements of index $\kappa' = j-\kappa$ and $\kappa' = j+1+\kappa$ in the two summations of the first equality. This purpose is easily checked as follows.

- If $j+i+1$ is odd, the replacement $\kappa' = i+j+1-\kappa$ implies $\Upsilon = (-1)^{i+j+1}\Upsilon$ and hence $\Upsilon = 0$.
- If $j+i+1$ is even, denoted by 2ℓ, a simple replacement of summation index again reduces

$$(-1)^{j-\ell}\Upsilon = \sum_{-\ell\le\kappa\le\ell} (-1)^\kappa \alpha_{\ell+\kappa}(m)\alpha_{\ell-\kappa}(m) = a_{\ell,\ell}^{(\ell)}(m),$$

  where the last step uses the second equation in (7.7). Since $\ell \le (2\zeta-1)/2 < \zeta$, it follows $a_{\ell,\ell}^{(\ell)}(m) = 0$ from the definition of the termination index of spatial discretization. This implies $\Upsilon = 0$ also.

Till now we sum up the above conclusions and complete the proof of this lemma. ☐

Due to (3.11) and (3.8), respectively, we can immediately obtain

$$\underline{\boldsymbol{Q}}(m;\vartheta)\underline{\boldsymbol{\Sigma}}(m) = \underline{\boldsymbol{\Phi}}(m)\underline{\boldsymbol{W}}(m;\vartheta), \quad \underline{\boldsymbol{\Phi}}(m)\underline{\boldsymbol{D}}(m) = \underline{\boldsymbol{\Sigma}}(m). \tag{7.8}$$

This implies $\underline{\boldsymbol{Q}}(m;\vartheta) = \underline{\boldsymbol{\Sigma}}(m)\underline{\boldsymbol{D}}(m)^{-1}\underline{\boldsymbol{W}}(m;\vartheta)\underline{\boldsymbol{\Sigma}}(m)^{-1}$. Lemma 7.1 and (7.5) deduce for any $0 \le i, j \le \zeta - 1$ that

$$z_{ij}(m;\vartheta) = \sum_{0\le\kappa\le i} 2(-1)^\kappa \alpha_{i-\kappa}(m)\pi_{\kappa,j}(m;\vartheta), \tag{7.9}$$

where

(7.10)
$$\pi_{\kappa,j}(m;\vartheta) = \sum_{0\le\ell\le ms-1} \alpha_{\ell+1+\kappa}(m)q_{\ell,j}(m;\vartheta)$$
$$= \left[\sum_{0\le\ell\le ms-1} \alpha_{\ell+1+\kappa}(m)\boldsymbol{e}_\ell^\top(m)\underline{\boldsymbol{\Sigma}}(m)\right]\cdot\left[\underline{\boldsymbol{D}}^{-1}(m)\underline{\boldsymbol{W}}(m;\vartheta)\right]\cdot\left[\underline{\boldsymbol{\Sigma}}(m)^{-1}\boldsymbol{e}_j(m)\right].$$

7.1.3. Simplification. In this subsection we want to set up an equivalent simplified expression of (7.10) by using the original data of the time marching as much as possible. We start from the calculation of $\underline{\boldsymbol{\Sigma}}(m)^{-1}$. By denoting (here and below we omit (m) in the matrix entry)

$$\underline{\boldsymbol{S}}(m) = \underline{\boldsymbol{I}}(m) - \underline{\boldsymbol{C}}(m)\underline{\boldsymbol{E}}(m) = \begin{pmatrix} 1 & & & & \\ -c_{11} & 1 & & & \\ -c_{21} & -c_{22} & 1 & & \\ \vdots & \vdots & & \ddots & \\ -c_{ms-1,1} & -c_{ms-1,2} & \cdots & -c_{ms-1,ms-1} & 1 \end{pmatrix},$$

the definition procedure of the temporal differences of stage solutions can be written into the matrix form

$$\left(\begin{array}{ccc|c} & \underline{\boldsymbol{\Sigma}}(m) & & \\ \hdashline \sigma_{ms,0} & \cdots & \sigma_{ms,ms-1} & \sigma_{ms,ms} \end{array}\right) = \left(\begin{array}{c|c} 1 & \\ \hdashline & \underline{\boldsymbol{\Phi}}(m) \end{array}\right) \left(\begin{array}{c|c} 1 & \\ \hdashline -\underline{\boldsymbol{C}}(m)\boldsymbol{e}_0(m) & \underline{\boldsymbol{S}}(m) \end{array}\right).$$

Recalling the definition of the evolution equation, the matrix inversion on both sides of the above identity yields

$$\left(\begin{array}{ccc|c} & \underline{\boldsymbol{\Sigma}}(m)^{-1} & & \\ \hdashline \alpha_0 & \cdots & \alpha_{ms-1} & \alpha_{ms} \end{array}\right) = \left(\begin{array}{c|c} 1 & \\ \hdashline \underline{\boldsymbol{S}}(m)^{-1}\underline{\boldsymbol{C}}(m)\boldsymbol{e}_0(m) & \underline{\boldsymbol{S}}(m)^{-1}\underline{\boldsymbol{D}}(m)\underline{\boldsymbol{\Sigma}}(m)^{-1} \end{array}\right),$$

where we have used (7.8) to get $\underline{\boldsymbol{\Phi}}(m)^{-1} = \underline{\boldsymbol{D}}(m)\underline{\boldsymbol{\Sigma}}(m)^{-1}$. Comparing with the matrices entries on both sides, we can achieve the following equalities for every column in the matrix $\underline{\boldsymbol{\Sigma}}(m)^{-1}$,

$$\underline{\boldsymbol{\Sigma}}(m)^{-1}\boldsymbol{e}_0(m) = [\underline{\boldsymbol{I}}(m) + \underline{\boldsymbol{E}}(m)\underline{\boldsymbol{S}}(m)^{-1}\underline{\boldsymbol{C}}(m)]\boldsymbol{e}_0(m) \stackrel{\text{def}}{=} \boldsymbol{q}(m), \tag{7.11a}$$

$$\underline{\boldsymbol{\Sigma}}(m)^{-1}\boldsymbol{e}_j(m) = \underbrace{\underline{\boldsymbol{E}}(m)\underline{\boldsymbol{S}}(m)^{-1}\underline{\boldsymbol{D}}(m)}_{\underline{\boldsymbol{K}}(m)}\underline{\boldsymbol{\Sigma}}(m)^{-1}\boldsymbol{e}_{j-1}(m), \quad j \geq 1, \tag{7.11b}$$

and for every evolution coefficient in (3.16),

$$\alpha_0(m) = \boldsymbol{e}_{ms-1}(m)^\top\underline{\boldsymbol{S}}(m)^{-1}\underline{\boldsymbol{C}}(m)\boldsymbol{e}_0(m), \tag{7.12a}$$

$$\alpha_j(m) = \underbrace{\boldsymbol{e}_{ms-1}(m)^\top\underline{\boldsymbol{S}}(m)^{-1}\underline{\boldsymbol{D}}(m)}_{\boldsymbol{p}^\top(m)}\underline{\boldsymbol{\Sigma}}(m)^{-1}\boldsymbol{e}_{j-1}(m), \quad j \geq 1. \tag{7.12b}$$

For those important parts in the above formulas, we need to investigate the relationship between one-step and multistep time marching.

To do that, we would like to use the (right) Kronecker product of matrices [23]. For example, it is easy to see

$$\boldsymbol{e}_0(m) = \hat{\boldsymbol{e}}_0 \otimes \boldsymbol{e}_0, \quad \boldsymbol{e}_{ms-1}(m)^\top = \hat{\boldsymbol{e}}_{m-1}^\top \otimes \boldsymbol{e}_{s-1}^\top, \quad \underline{\boldsymbol{I}}(m) = \hat{\underline{\boldsymbol{I}}} \otimes \underline{\boldsymbol{I}},$$

which implies $\underline{\boldsymbol{E}}(m) = \hat{\underline{\boldsymbol{I}}} \otimes \underline{\boldsymbol{E}} + \hat{\underline{\boldsymbol{E}}} \otimes \boldsymbol{e}_0\boldsymbol{e}_{s-1}^\top$. Due to the definition (3.3), we derive

$$\underline{\boldsymbol{C}}(m) = \hat{\underline{\boldsymbol{I}}} \otimes \underline{\boldsymbol{C}}, \quad \underline{\boldsymbol{D}}(m) = \frac{1}{m}\hat{\underline{\boldsymbol{I}}} \otimes \underline{\boldsymbol{D}}, \quad \underline{\boldsymbol{W}}(m;\vartheta) = \frac{1}{m}\hat{\underline{\boldsymbol{I}}} \otimes \underline{\boldsymbol{W}}(\vartheta), \tag{7.13}$$

where $\underline{\boldsymbol{W}}(\vartheta) = \underline{\boldsymbol{W}}(1;\vartheta)$. Further, by some lengthy and tedious matrices manipulations, we can get the following important identities

$$\underline{\boldsymbol{S}}(m)^{-1} = \hat{\underline{\boldsymbol{L}}} \otimes \underline{\boldsymbol{S}}^{-1}\underline{\boldsymbol{C}}\boldsymbol{e}_0\boldsymbol{e}_{s-1}^\top\underline{\boldsymbol{S}}^{-1} + \hat{\underline{\boldsymbol{I}}} \otimes \underline{\boldsymbol{S}}^{-1}, \tag{7.14a}$$

$$\underline{\boldsymbol{K}}(m) = \frac{1}{m}\Big[\hat{\underline{\boldsymbol{L}}} \otimes \boldsymbol{q}\boldsymbol{p}^\top + \hat{\underline{\boldsymbol{I}}} \otimes \underline{\boldsymbol{E}}\,\underline{\boldsymbol{S}}^{-1}\underline{\boldsymbol{D}}\Big], \tag{7.14b}$$

$$\boldsymbol{p}(m)^\top = \frac{1}{m}\hat{\mathbf{1}} \otimes \boldsymbol{p}^\top, \tag{7.14c}$$

$$\boldsymbol{q}(m) = \hat{\mathbf{1}} \otimes \boldsymbol{q}. \tag{7.14d}$$

In this process, we have used some simple conclusions

$$\hat{\underline{\boldsymbol{E}}} + \hat{\underline{\boldsymbol{E}}}\,\hat{\underline{\boldsymbol{L}}} = \hat{\underline{\boldsymbol{L}}}, \quad \hat{\boldsymbol{e}}_{m-1}^\top + \hat{\boldsymbol{e}}_{m-1}^\top \hat{\underline{\boldsymbol{L}}} = \hat{\mathbf{1}}^\top, \quad \hat{\boldsymbol{e}}_0 + \hat{\underline{\boldsymbol{L}}}\hat{\boldsymbol{e}}_0 = \hat{\mathbf{1}},$$

and an important identity, as a corollary of (7.12a) and $\alpha_0(m) = 1$,

$$\boldsymbol{e}_{ms-1}^\top(m)\underline{\boldsymbol{S}}(m)^{-1}\underline{\boldsymbol{C}}(m)\boldsymbol{e}_0(m) = 1. \tag{7.15}$$

Limited by the length of this paper, we omit the detailed verifications for (7.14).

Based on the above conclusions, we are ready to simplify formula (7.10). An induction process for (7.11) yields the following identity

$$\underline{\boldsymbol{\Sigma}}(m)^{-1}\boldsymbol{e}_j(m) = \underline{\boldsymbol{K}}(m)^j\boldsymbol{q}(m) = \underline{\boldsymbol{K}}(m)^j(\hat{\mathbf{1}} \otimes \boldsymbol{q}), \quad j \geq 0, \tag{7.16}$$

where (7.14d) is used at the last step. The corresponding matrix expression is

$$\underline{\boldsymbol{\Sigma}}(m)^{-1}\underline{\boldsymbol{E}}(m) = \underline{\boldsymbol{K}}(m)\underline{\boldsymbol{\Sigma}}(m)^{-1}. \tag{7.17}$$

Since $\sum_{0\leq\ell\leq ms-1}\boldsymbol{e}_{\ell+\kappa}(m)^\top\boldsymbol{e}_\ell(m)^\top = \underline{\boldsymbol{E}}(m)^\kappa$, we use (7.12b) to get for any $\kappa \geq 0$ that

$$\begin{aligned}\sum_{0\leq\ell\leq ms-1}\alpha_{\ell+1+\kappa}(m)\boldsymbol{e}_\ell(m)^\top\underline{\boldsymbol{\Sigma}}(m) &= \boldsymbol{p}(m)^\top\underline{\boldsymbol{\Sigma}}(m)^{-1}\underline{\boldsymbol{E}}(m)^\kappa\underline{\boldsymbol{\Sigma}}(m)\\ &= \boldsymbol{p}(m)^\top[\underline{\boldsymbol{\Sigma}}(m)^{-1}\underline{\boldsymbol{E}}(m)\underline{\boldsymbol{\Sigma}}(m)]^\kappa = \boldsymbol{p}(m)^\top\underline{\boldsymbol{K}}(m)^\kappa = \frac{1}{m}\left(\hat{\mathbf{1}}^\top \otimes \boldsymbol{p}^\top\right)\underline{\boldsymbol{K}}(m)^\kappa,\end{aligned} \tag{7.18}$$

where (7.17) and (7.14c) are respectively used at the last two steps. With the help of (7.13), substituting (7.16) and (7.18) into (7.10) yields a simplification expression

$$\pi_{\kappa,j}(m;\vartheta) = \frac{1}{m}\Big(\hat{\mathbf{1}}^\top \otimes \boldsymbol{p}^\top\Big)\underline{\boldsymbol{K}}(m)^\kappa\Big(\hat{\underline{\boldsymbol{I}}} \otimes \underline{\boldsymbol{D}}^{-1}\underline{\boldsymbol{W}}(\vartheta)\Big)\underline{\boldsymbol{K}}(m)^j\Big(\mathbf{1} \otimes \boldsymbol{q}\Big). \tag{7.19}$$

This ends this subsection.

7.2. Proof of Lemma 3.3. Noticing (3.14) and $\alpha_1 = 1$, it follows from (3.28) and (7.10) that $\Theta(m) = \vartheta + \pi_{00}(m;\vartheta)$ for any ϑ. Then (7.19) implies that

$$\Theta(m) = \vartheta + \frac{1}{m}\Big(\hat{\mathbf{1}}^\top \otimes \boldsymbol{p}^\top\Big)\Big(\hat{\underline{\boldsymbol{I}}} \otimes \underline{\boldsymbol{D}}^{-1}\underline{\boldsymbol{W}}(\vartheta)\Big)\Big(\hat{\mathbf{1}} \otimes \boldsymbol{q}\Big) = \vartheta + \boldsymbol{p}^\top\underline{\boldsymbol{D}}^{-1}\underline{\boldsymbol{W}}(\vartheta)\boldsymbol{q}, \tag{7.20}$$

due to the simple fact $\hat{\mathbf{1}}^\top\hat{\underline{\boldsymbol{I}}}\hat{\mathbf{1}} = m$. This completes the proof of Lemma 3.3.

Taking $m = 1$ and $\vartheta = \Theta$ in (7.20), we use Lemma 3.3 to get

$$\boldsymbol{p}^\top\underline{\boldsymbol{D}}^{-1}\underline{\boldsymbol{W}}(\Theta)\boldsymbol{q} = 0. \tag{7.21}$$

This property reflects the essence of the averaged numerical flux parameter, and plays an important role in the proof of Lemma 3.4.

REMARK 7.1. *Assume that the numerical flux parameters are the same at each time marching, and alternatively taken from two numbers θ_1 and θ_2 for different n. By (7.20) and (7.21), a simple manipulation shows $\Theta = (\theta_1 + \theta_2)/2$. This clearly reflects the meaning of the averaged numerical flux parameter.*

7.3. Proof of Lemma 3.4. For convenience of notations, we use a generic notation C to denote a positive constant independent of m.

Recalling the proof of [24, Proposition 3.3], we have for $0 \le i, j \le \zeta - 1$ that

$$\left| b^{\star}_{ij}(m) - \frac{2}{i!j!(i+j+1)} \right| \le \frac{C}{m}, \tag{7.22}$$

and we emphasize that $\{\frac{2}{i!j!(i+j+1)}\}_{0\le i,j\le\zeta-1}$ forms a symmetric positive definite matrix. Since the averaged numerical flux parameter is assumed to be $\Theta > 1/2$, noticing (7.2) and (7.9), it is sufficient to prove this lemma by showing for $0 \le \kappa, j \le \zeta - 1$ that

$$|\pi_{\kappa,j}(m;\Theta)| \le \frac{C}{m}. \tag{7.23}$$

Here we have used the fact that $\alpha_{i-\kappa}(m)$ is bounded independent of m, since [24, inequality (3.16)] has shown $|\alpha_{i'}(m) - 1/i'!| \le C/m^r$ for $0 \le i' \le 2\zeta - 1$.

Denote $\pi_{\kappa,j} = \pi_{\kappa,j}(m;\Theta)$ and $\underline{\boldsymbol{W}} = \underline{\boldsymbol{W}}(\Theta)$ for simplicity. Below we prove (7.23) for different cases, where (7.21) plays an important role to well control the accumulation and growth as m goes to infinity.

- If $\kappa = j = 0$, we have $\pi_{0,0} = (\hat{\mathbf{1}}^\top \underline{\hat{\boldsymbol{I}}} \hat{\mathbf{1}}) \otimes (\boldsymbol{p}^\top \underline{\boldsymbol{D}}^{-1} \underline{\boldsymbol{W}} \boldsymbol{q}) = 0$, due to (7.21).
- If $\kappa > 0$ and $j > 0$, we have

  $$\pi_{\kappa,j} = \frac{1}{m}\Big(\hat{\mathbf{1}}^\top \otimes \boldsymbol{p}^\top\Big)[\underline{\boldsymbol{K}}(m)]^{\kappa-1}\boldsymbol{\Pi}_{\kappa,j}(m)[\underline{\boldsymbol{K}}(m)]^{j-1}\Big(\hat{\mathbf{1}} \otimes \boldsymbol{q}\Big), \tag{7.24}$$

  where

  $$\boldsymbol{\Pi}_{\kappa,j}(m) = \underline{\boldsymbol{K}}(m)\Big(\underline{\hat{\boldsymbol{I}}} \otimes \underline{\boldsymbol{D}}^{-1}\underline{\boldsymbol{W}}\Big)\underline{\boldsymbol{K}}(m).$$

  Substituting (7.14b) into this formula and then using (7.21) to eliminate the term involving $\underline{\hat{\boldsymbol{L}}}^2$. After some manipulations we yield

  $$\begin{aligned}\boldsymbol{\Pi}_{\kappa,j}(m) = {}& \frac{1}{m^2}\underline{\hat{\boldsymbol{L}}} \otimes [\boldsymbol{q}\boldsymbol{p}^\top \underline{\boldsymbol{D}}^{-1}\underline{\boldsymbol{W}}\underline{\boldsymbol{E}\boldsymbol{S}}^{-1}\underline{\boldsymbol{D}} + \underline{\boldsymbol{E}\boldsymbol{S}}^{-1}\underline{\boldsymbol{W}}\boldsymbol{q}\boldsymbol{p}^\top] \\ & + \frac{1}{m^2}\underline{\hat{\boldsymbol{I}}} \otimes \underline{\boldsymbol{E}\boldsymbol{S}}^{-1}\underline{\boldsymbol{W}}\underline{\boldsymbol{E}\boldsymbol{S}}^{-1}\underline{\boldsymbol{D}}.\end{aligned}$$

  The row norms for all matrices (including the row vectors and column vectors) do not depend on m, except that $\|\underline{\hat{\boldsymbol{L}}}\|_\infty = m - 1$. Hence we have

  $$\|\boldsymbol{\Pi}_{\kappa,j}(m)\|_\infty \le \frac{C}{m}.$$

  Noticing $\|\frac{1}{m}(\hat{\mathbf{1}}^\top \otimes \boldsymbol{p}^\top)\|_\infty \le C$ and $\|\underline{\boldsymbol{K}}(m)\|_\infty \le C$, we get from (7.24) what we want to prove.
- If $\kappa = 0$ and $j > 0$, we have $\pi_{0,j} = \frac{1}{m}\boldsymbol{\Pi}_{0,j}(m)[\underline{\boldsymbol{K}}(m)]^{j-1}(\hat{\mathbf{1}} \otimes \boldsymbol{q})$ with

  $$\boldsymbol{\Pi}_{0,j}(m) = \Big(\hat{\mathbf{1}}^\top \otimes \boldsymbol{p}^\top\Big)\Big(\underline{\hat{\boldsymbol{I}}} \otimes \underline{\boldsymbol{D}}^{-1}\underline{\boldsymbol{W}}\Big)\underline{\boldsymbol{K}}(m) = \frac{1}{m}\hat{\mathbf{1}}^\top \otimes \boldsymbol{p}^\top \underline{\boldsymbol{D}}^{-1}\underline{\boldsymbol{W}}\underline{\boldsymbol{E}\boldsymbol{S}}^{-1}\underline{\boldsymbol{D}},$$

  by some manipulations with the help of (7.14b) and (7.21). The remaining proof follows the same line as above, hence is omitted.
- If $\kappa > 0$ and $j = 0$, we have $\pi_{\kappa,0} = \frac{1}{m}(\hat{\mathbf{1}}^\top \otimes \boldsymbol{p}^\top)[\underline{\boldsymbol{K}}(m)]^{\kappa-1}\boldsymbol{\Pi}_{\kappa,0}(m)$, where

  $$\boldsymbol{\Pi}_{\kappa,0}(m) = \underline{\boldsymbol{K}}(m)(\underline{\hat{\boldsymbol{I}}} \otimes \underline{\boldsymbol{D}}^{-1}\underline{\boldsymbol{W}})(\hat{\mathbf{1}} \otimes \boldsymbol{q}) = \hat{\mathbf{1}} \otimes \underline{\boldsymbol{E}\boldsymbol{S}}^{-1}\underline{\boldsymbol{W}}\boldsymbol{q},$$

  with the help of (7.14b) and (7.21). Then we can prove (7.24) as above.

Summing up the above conclusions, we verify (7.23) and then prove this lemma.

7.4. Proof of Propositions 3.1 and 3.2. Taking $\vartheta = 0$ in (7.20) and substituting the definition of $\boldsymbol{p}^\top$ and $\boldsymbol{q}$, we have

$$\Theta = \boldsymbol{e}_{s-1}^\top \underline{\boldsymbol{S}}^{-1} \underline{\boldsymbol{W}}(0)(\underline{\boldsymbol{I}} + \underline{\boldsymbol{E}}\underline{\boldsymbol{S}}^{-1}\underline{\boldsymbol{C}})\boldsymbol{e}_0. \tag{7.25}$$

This identity will be used below.

Since we have assumed $c_{\ell\kappa} \geq 0$ for any ℓ and κ in this paper, we can conclude that all entries of $\underline{\boldsymbol{S}}^{-1}$ are non-negative by using the simple fact

$$\underline{\boldsymbol{S}}^{-1} = (\underline{\boldsymbol{I}} - \underline{\boldsymbol{E}}\underline{\boldsymbol{C}})^{-1} = \underline{\boldsymbol{I}} + \sum_{1\leq i\leq s-1} (\underline{\boldsymbol{E}}\underline{\boldsymbol{C}})^i.$$

Hence we can conclude from (7.25) that Θ is a non-negative linear combination of the entries of $\underline{\boldsymbol{W}}(0) = \{d_{\ell\kappa}\theta_{\ell\kappa}\}_{0\leq \ell,\kappa\leq s-1}$. This proves Proposition 3.1.

For the LWDG method with the time marching coefficients (2.10), we have $\underline{\boldsymbol{S}} = \underline{\boldsymbol{I}}$ and we get from (7.25) that

$$\Theta = \boldsymbol{e}_{s-1}^\top \underline{\boldsymbol{W}}(0)\boldsymbol{e}_0 = d_{s-1,0}\theta_{s-1,0} = \theta_{s-1,0}, \tag{7.26}$$

since $\underline{\boldsymbol{I}} + \underline{\boldsymbol{E}}\underline{\boldsymbol{S}}^{-1}\underline{\boldsymbol{C}} = \underline{\boldsymbol{I}} + \underline{\boldsymbol{E}}\underline{\boldsymbol{C}} = \underline{\boldsymbol{I}}$. This completes the proof of Proposition 3.2.

REFERENCES

[1] J. Ai, Y. Xu, C.-W. Shu, and Q. Zhang, *L^2 error estimate to smooth solutions of high order Runge-Kutta discontinuous Galerkin method for scalar nonlinear conservation laws with and without sonic points*, SIAM J. Numer. Anal., 60 (2022), pp. 1741–1773, https://doi.org/10.1137/21M1435495.

[2] G. Chavent and B. Cockburn, *The local projection P^0P^1-discontinuous-Galerkin finite element method for scalar conservation laws*, RAIRO Modél. Math. Anal. Numér., 23 (1989), pp. 565–592, https://doi.org/10.1051/m2an/1989230405651.

[3] Y. Cheng, X. Meng, and Q. Zhang, *Application of generalized Gauss-Radau projections for the local discontinuous Galerkin method for linear convection-diffusion equations*, Math. Comp., 86 (2017), pp. 1233–1267, https://doi.org/10.1090/mcom/3141.

[4] P. G. Ciarlet, *The finite element method for elliptic problems*, North-Holland Publishing Co., Amsterdam-New York-Oxford, 1978. Studies in Mathematics and its Applications, Vol. 4.

[5] B. Cockburn, S. Hou, and C.-W. Shu, *The Runge-Kutta local projection discontinuous Galerkin finite element method for conservation laws. IV. The multidimensional case*, Math. Comp., 54 (1990), pp. 545–581, https://doi.org/10.2307/2008501.

[6] B. Cockburn, S. Y. Lin, and C.-W. Shu, *TVB Runge-Kutta local projection discontinuous Galerkin finite element method for conservation laws. III. One-dimensional systems*, J. Comput. Phys., 84 (1989), pp. 90–113, https://doi.org/10.1016/0021-9991(89)90183-6.

[7] B. Cockburn and C.-W. Shu, *TVB Runge-Kutta local projection discontinuous Galerkin finite element method for conservation laws. II. General framework*, Math. Comp., 52 (1989), pp. 411–435, https://doi.org/10.2307/2008474.

[8] B. Cockburn and C.-W. Shu, *The Runge-Kutta local projection P^1-discontinuous-Galerkin finite element method for scalar conservation laws*, RAIRO Modél. Math. Anal. Numér., 25 (1991), pp. 337–361, https://doi.org/10.1051/m2an/1991250303371.

[9] B. Cockburn and C.-W. Shu, *The Runge-Kutta discontinuous Galerkin method for conservation laws. V. Multidimensional systems*, J. Comput. Phys., 141 (1998), pp. 199–224, https://doi.org/10.1006/jcph.1998.5892.

[10] B. Cockburn and C.-W. Shu, *Runge-Kutta discontinuous Galerkin methods for convection-dominated problems*, J. Sci. Comput., 16 (2001), pp. 173–261, https://doi.org/10.1023/A:1012873910884.

[11] S. Gottlieb and S. J. Ruuth, *Optimal strong-stability-preserving time-stepping schemes with fast downwind spatial discretizations*, J. Sci. Comput., 27 (2006), pp. 289–303, https://doi.org/10.1007/s10915-005-9054-8.

[12] S. Gottlieb and C.-W. Shu, *Total variation diminishing Runge-Kutta schemes*, Math. Comp., 67 (1998), pp. 73–85, https://doi.org/10.1090/S0025-5718-98-00913-2.

[13] W. Guo, J.-M. Qiu, and J. Qiu, *A new Lax-Wendroff discontinuous Galerkin method with superconvergence*, J. Sci. Comput., 65 (2015), pp. 299–326, https://doi.org/10.1007/s10915-014-9968-0.

[14] J. Qiu and Q. Zhang, *Stability, error estimate and limiters of discontinuous Galerkin methods*, in Handbook of Numerical Methods for Hyperbolic Problems, vol. 17 of Handbook of Numerical Analysis, Elsevier, 2016, pp. 147–171, https://doi.org/10.1016/bs.hna.2016.06.001.

[15] S. J. Ruuth, *Global optimization of explicit strong-stability-preserving Runge-Kutta methods*, Math. Comp., 75 (2006), pp. 183–207, https://doi.org/10.1090/S0025-5718-05-01772-2.

[16] S. J. Ruuth and R. J. Spiteri, *Two barriers on strong-stability-preserving time discretization methods*, J. Sci. Comput., 17 (2002), pp. 211–220, https://doi.org/10.1023/A:1015156832269.

[17] S. J. Ruuth and R. J. Spiteri, *High-order strong-stability-preserving Runge-Kutta methods with downwind-biased spatial discretizations*, SIAM J. Numer. Anal., 42 (2004), pp. 974–996, https://doi.org/10.1137/S0036142902419284.

[18] C.-W. Shu, *Total-variation-diminishing time discretizations*, SIAM J. Sci. Statist. Comput., 9 (1988), pp. 1073–1084, https://doi.org/10.1137/0909073.

[19] C.-W. Shu, *Discontinuous Galerkin methods: general approach and stability*, in Numerical solutions of partial differential equations, Adv. Courses Math. CRM Barcelona, Birkhäuser, Basel, 2009, pp. 149–201.

[20] C.-W. Shu, *Discontinuous Galerkin methods for time-dependent convection dominated problems: basics, recent developments and comparison with other methods*, in Building bridges: connections and challenges in modern approaches to numerical partial differential equations, vol. 114 of Lect. Notes Comput. Sci. Eng., Springer, 2016, pp. 369–397.

[21] C.-W. Shu and S. Osher, *Efficient implementation of essentially nonoscillatory shock-capturing schemes*, J. Comput. Phys., 77 (1988), pp. 439–471, https://doi.org/10.1016/0021-9991(88)90177-5.

[22] Z. Sun and C.-W. Shu, *Stability analysis and error estimates of Lax-Wendroff discontinuous Galerkin methods for linear conservation laws*, ESAIM Math. Model. Numer. Anal., 51 (2017), pp. 1063–1087, https://doi.org/10.1051/m2an/2016049.

[23] C. F. Van Loan, *The ubiquitous Kronecker product*, J. Comput. Appl. Math., 123 (2000), pp. 85–100, https://doi.org/10.1016/S0377-0427(00)00393-9.

[24] Y. Xu, X. Meng, C.-W. Shu, and Q. Zhang, *Superconvergence analysis of the Runge-Kutta discontinuous Galerkin methods for a linear hyperbolic equation*, J. Sci. Comput., 84 (2020), https://doi.org/10.1007/s10915-020-01274-1.

[25] Y. Xu, C.-W. Shu, and Q. Zhang, *Error estimate of the fourth-order Runge–Kutta discontinuous Galerkin methods for linear hyperbolic equations*, SIAM J. Numer. Anal., 58 (2020), pp. 2885–2914, https://doi.org/10.1137/19M1280077.

[26] Y. Xu and Q. Zhang, *Superconvergence analysis of the Runge-Kutta discontinuous Galerkin method with upwind-biased numerical flux for two dimensional linear hyperbolic equation*, Commun. Appl. Math. Comput., 4 (2022), pp. 319–352, https://doi.org/10.1007/s42967-020-00116-z.

[27] Y. Xu, Q. Zhang, C.-W. Shu, and H. Wang, *The L^2-norm stability analysis of Runge-Kutta discontinuous Galerkin methods for linear hyperbolic equations*, SIAM J. Numer. Anal., 57 (2019), pp. 1574–1601, https://doi.org/10.1137/18M1230700.

[28] Y. Xu, D. Zhao, and Q. Zhang, *Local error estimates for Runge-Kutta discontinuous Galerkin methods with upwind-biased numerical fluxes for a linear hyperbolic equation in one-dimension with discontinuous initial data*, J. Sci. Comput., 91 (2022), https://doi.org/10.1007/s10915-022-01793-z.

[29] Q. Zhang and C.-W. Shu, *Error estimates to smooth solutions of Runge-Kutta discontinuous Galerkin methods for scalar conservation laws*, SIAM J. Numer. Anal., 42 (2004), pp. 641–666, https://doi.org/10.1137/S0036142902404182.

[30] Q. Zhang and C.-W. Shu, *Stability analysis and a priori error estimates of the third order explicit Runge-Kutta discontinuous Galerkin method for scalar conservation laws*, SIAM J. Numer. Anal., 48 (2010), pp. 1038–1063, https://doi.org/10.1137/090771363.